Vertical-axis rotations determined from paleomagnetism of Mesozoic and Cenozoic strata of the Bolivian Andes

David R. Richards[1] and Robert F. Butler[2]

Department of Geosciences, University of Arizona, Tucson, Arizona, USA

Thierry Sempere[3]

Institut de Recherche pour le Développement (IRD), Lima, Peru

[1] Thermal demagnetization and principal component analysis allowed determination of characteristic remanent magnetization (ChRM) directions from 256 sites at 22 localities in Mesozoic and Cenozoic sedimentary strata of the Bolivian Altiplano and Eastern Cordillera. An inclination-only fold test of site-mean ChRM directions from Cenozoic units (principally the Santa Lucía Formation) indicates optimum unfolding at 97.1% unfolding, consistent with a primary origin for the ChRM. For Mesozoic strata, optimum unfolding occurred at 89.2%, perhaps indicating secondary remagnetization at some locations. For Cenozoic units, comparison of locality-mean directions with expected paleomagnetic directions indicates vertical-axis rotations from 33° counterclockwise to 24° clockwise. Euler pole analysis of along-strike variation in crustal shortening within the Subandean and Interandean zones indicates 18° clockwise rotation south of the axis of curvature of the Bolivian Andes and 6° counterclockwise rotation northwest of the axis during the past 10 m.y. Along-strike variation of shortening within the Eastern Cordillera indicates 8° clockwise rotation south of the axis and 8° counterclockwise rotation northwest of the axis from 35 to 10 Ma. These vertical-axis rotations produced by along-strike variations in crustal shortening during development of the Bolivian fold-thrust belt agree well with observed rotations determined from paleomagnetism of Cenozoic rocks in the Eastern Cordillera and in the Subandean and Interandean zones. However, local rotations are required to account for complex rotations in the Cochabamba Basin and within the Altiplano. The curvature of the Bolivian Andes has been progressively enhanced during Cenozoic fold-thrust belt deformation.   INDEX TERMS: 1525 Geomagnetism and Paleomagnetism: Paleomagnetism applied to tectonics (regional, global); 8102 Tectonophysics: Continental contractional orogenic belts; 8164 Tectonophysics: Stresses—crust and lithosphere; 9360 Information Related to Geographic Region: South America; 9604 Information Related to Geologic Time: Cenozoic; KEYWORDS: tectonics, paleomagnetism, South America, Cenozoic, Bolivia

1. Introduction

[2] The Andean Cordillera has been built along an active continental margin by processes directly related to the subduction of the oceanic Nazca plate below the South American continent. Along the length of the mountain chain, the Andes present variations in width, altitude, geology, and crustal thickness. In the curved segment known as the "Bolivian Orocline" (12°–28°S latitude; [Isacks, 1988; Gephart, 1994]), the width of the orogen between the Peru–Chile trench and the Subandean front reaches 850 km and the crustal thickness is locally over 70 km [Beck et al., 1996; Yuan et al., 2002] (Figure 1). The second largest continental plateau on Earth, the Altiplano of southern Peru and Bolivia and the Puna Plateau of northern Chile and northwestern Argentina, is found in the Bolivian Orocline. There is broad consensus that the Bolivian Eastern Cordillera and Subandean belt resulted from crustal shortening, whereas the origin and structure of the Altiplano is debated [Baby et al., 1997; DeCelles and Horton, 2003; McQuarrie, 2002a; Sempere et al., 2002; Husson and Sempere, 2003].

[3] Deformation within the Central Andes has included vertical-axis rotations on a range of scales. Syntheses of vertical-axis rotations documented by paleomagnetism have been presented by Isacks [1988], Beck et al. [1994], Randall [1998], and Somoza [1998]. Both large-scale bending of the

---

[1]Now at Midland Valley Inc., Golden, Colorado, USA.
[2]Now at Department of Chemistry and Physics, University of Portland, Portland, Oregon, USA.
[3]Now at Laboratoire des Mécanismes et Transferts en Géologie, Université Paul Sabatier, Toulouse, France.
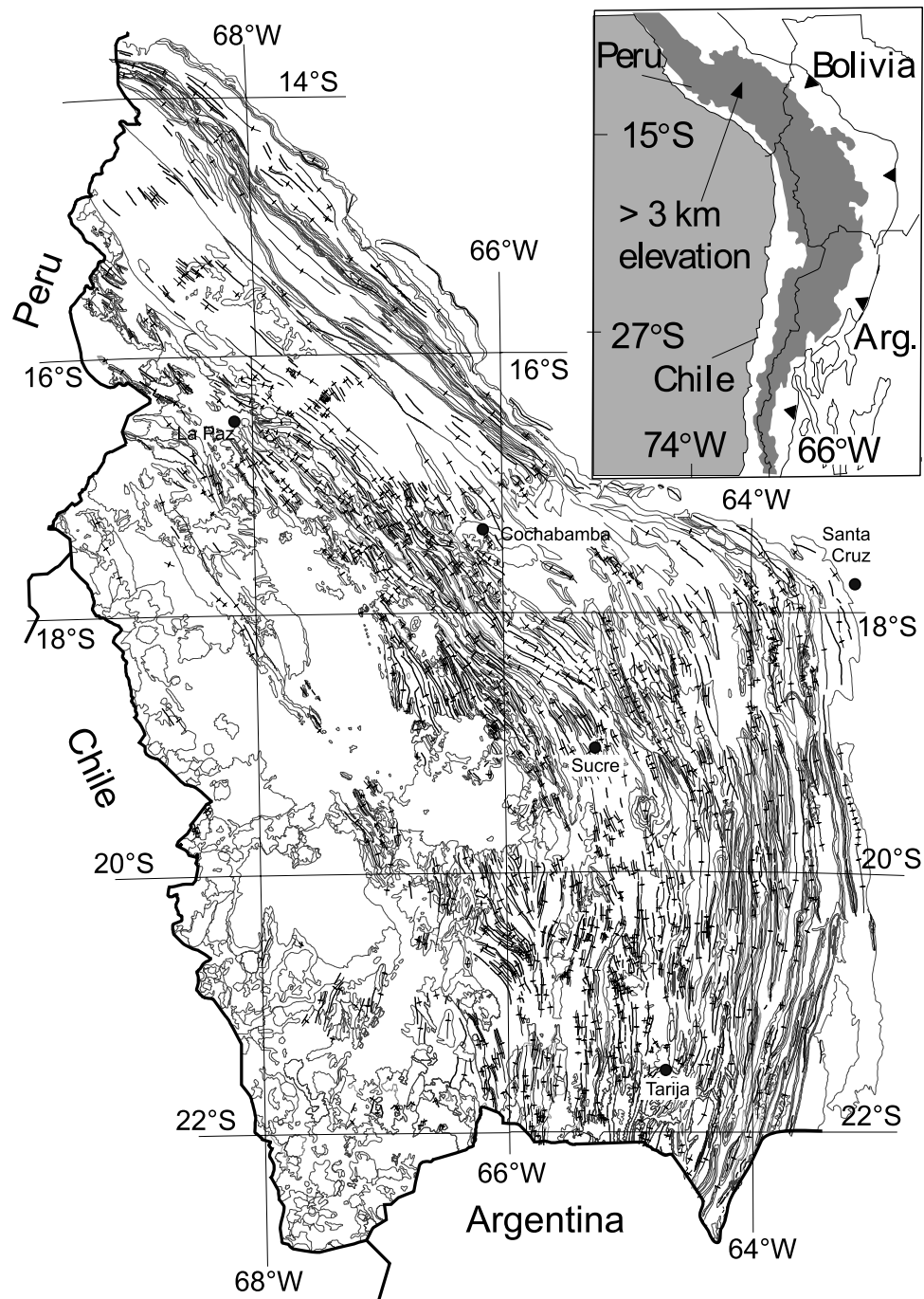
Figure 1. Major geologic structures of the Altiplano, Eastern Cordillera, and Subandean and Interandean zone of Bolivia. Geologic contacts are shown in gray lines; fold axes of synclines are shown decorated with cross marks; anticlinal fold axes are undecorated and shown in heavier lines. Inset map shows central Andes with elevations >3000 m shaded. Geologic data are from 1:1,000,000 scale Mapa Geológico de Bolivia geographic information databases from Servicio Nacional de Geología y Minería and Yacimientos Petroliferos Fiscales Bolivianos.

Central Andes and ball-bearing or rotating-panel vertical-axis rotations of crustal blocks (10–20 km dimensions) have affected the forearc region of southern Peru and northern Chile [*Beck et al.*, 1994; *May and Butler*, 1985]. Recent studies of vertical-axis rotations in these coastal regions include *Beck* [1987, 1988, 1998], *Randall* [1998], *Randall et al.* [2001], *Rousse et al.* [2002], *Somoza et al.* [1996, 1999] and *Somoza and Tomlinson* [2002]. The number of paleomagnetic results from the forearc region has increased substantially during the past decade. These data clearly indicate the importance of local block rotations perhaps resulting from distributed shear of the South American continental margin by oblique subduction [*McQuarrie*, 2002a].

[4] A complete analysis of the Central Andes of Bolivia, northern Chile, northwest Argentina, and Peru is beyond the scope of this paper. Instead we focus on the Bolivian Andes. The Bolivian Orocline is not an orocline in the sense of an originally straight mountain system that has been bent into a curved map pattern as discussed by *Carey* [1955]. The Bolivian Orocline is essentially a megasalient in the orogen that displays along-strike variations in the amount of crustal shortening [*Marshak*, 1988]. Analysis of vertical-axis rotations in the Bolivian Orocline as the result of enhanced curvature of the mountain belt associated with crustal shortening and building of the Altiplano and Puna plateaus was initiated by *Isacks* [1988]. Analyses of paleomagnetically determined vertical-axis rotations within the Bolivian Andes have been presented by *MacFadden et al.* [1990, 1995], *Butler et al.* [1995], *Roperch et al.* [2000], and *Lamb* [2001a, 2001b]. In this paper, we present paleomagnetic data from Paleogene and Mesozoic sedimentary rocks at a large number of localities within the Altiplano and Eastern Cordillera of Bolivia. We then analyze resulting determinations of vertical-axis rotations within the Bolivian fold-thrust belt using recent structural geologic studies that estimate along-strike variations in crustal shortening [*Baby et al.*, 1997; *Kley*, 1999; *Kley and Monaldi*, 1998; *Kley et al.*, 1999; *McQuarrie*, 2002a, 2002b].

2. Paleomagnetic Sampling and Methods

[5] Paleomagnetic samples were collected from numerous outcrops of Mesozoic and Cenozoic red sedimentary strata within the Eastern Cordillera and the eastern portion of the Altiplano of Bolivia. Lithostratigraphy and geochronology of the sampled formations are taken from *Sempere et al.* [1997, 2002]. Uncertainties in age assignments of the sampled formations do not have major impact on interpretations of the paleomagnetic data. For example, the Potoco (Camargo) Formation is considered by *Sempere et al.* [1997] to be latest Paleocene-Oligocene on the basis of the paleontological data, whereas *DeCelles and Horton* [2003] suggest that its base is not older than Oligocene. Using reference paleomagnetic poles from *Besse and Courtillot* [2002], the expected paleomagnetic declination at Camargo changes by only 2.2° between 50 Ma and 30 Ma so vertical-axis rotation inferred from the observed paleomagnetic declination of the Potoco (Camargo) Formation is little affected by the age uncertainty.

[6] We use the term "paleomagnetic locality" to indicate an area (dimensions usually <10 km) from which one or several stratigraphic sections were sampled. Localities are illustrated on the map in Figure 2. Localities were carefully selected with two major considerations: (1) Sampled stratigraphic sections were 10s to 100s of meters in stratigraphic thickness so that the multiple paleomagnetic sites would provide adequate sampling of geomagnetic secular variation. (2) Recognizing the potential difficulty accounting for plunge of folds and attendant uncertainty in locality-mean paleomagnetic declination, sampling localities favored the central portions of large folds remote from the noses of these structures where plunge correction is critical. Accordingly no plunge corrections have been applied to observed paleomagnetic directions. Despite careful selection of sampling localities, it is not always possible to know with

certainty whether plunge corrections are required even in what appear to be straightforward structural geologic settings. In presentation of paleomagnetic data and discussion of results below, we provide cautionary notes about vertical-axis rotations determined from localities with steeply dipping strata.

[7] Paleomagnetic sampling was done using methods described by *Butler* [1992]. At each paleomagnetic site, oriented samples were collected either from a single sedimentary bed or several adjacent beds with cumulative stratigraphic thickness <1 m. At most sites, at least eight oriented samples (mostly cored samples) were collected at each site. Exceptions include the four localities collected during magnetostratigraphic studies (Laguna Umayo, La Palca, Sucusuma, and Tiupampa) where four oriented samples were collected at each site [*Butler et al.*, 1995; *Sempere et al.*, 1997; *Sigé et al.*, 2004]. Site-mean directions from those localities were illustrated by *Butler et al.* [1995] but were not tabulated in that publication; site-mean directions from Laguna Umayo have subsequently been tabulated by *Sigé et al.* [2004]. For the La Palca, Sucusuma, and Tiupampa localities, site-mean directions that pass the selection criteria outlined below are tabulated here for completeness.

[8] All samples were stored, thermally demagnetized and measured in a magnetically shielded room with average field intensity below 200 nannoTesla (nT). After initial measurement of natural remanent magnetization (NRM), samples were thermally demagnetized at 10 to 20 temperatures from 50°C to 700°C in furnaces with magnetic field <20 nT in the sample region. Representative behaviors during thermal demagnetization are illustrated in Figure 3. As anticipated for red sedimentary rocks, unblocking temperatures are often concentrated near the 680°C Néel temperature for hematite. For sites that failed to provide an acceptable site-mean ChRM direction, erratic direction and intensity changes were often observed at demagnetization temperatures above 500°C (Figure 3g). For sites yielding an acceptable site-mean ChRM direction, sample ChRM directions were usually isolated in the 550°C to 680°C interval.

[9] Results from at least four successive temperatures were analyzed by principal component analysis [*Kirschvink*, 1980] to determine sample characteristic remanent magnetization (ChRM) directions. Samples yielding maximum angular deviation (MAD) >15° were rejected from further analysis. Site-mean ChRM directions were calculated using methods of *Fisher* [1953] and sample ChRM directions more than two angular standard deviations from the initial site-mean direction were rejected prior to final site-mean calculation. Sites with less than four sample ChRM directions and site-mean directions with $\alpha_{95} > 25°$ were rejected. Only two included sites have $\alpha_{95} > 20°$ and the vast majority of sites have $\alpha_{95} < 10°$. When both normal and reverse polarity site-mean directions are present from a locality, the reversals test of *McFadden and McElhinny* [1990] was applied.

[10] Almost all strata are in homoclinal sections or in outcrops where bedding attitude changes are minor. With only one exception described below, the fold test was indeterminate using either the methods described by *McFadden* [1990] or *Watson and Enkin* [1993]. Following presentation of results from each locality, results of regional inclination-only fold tests are presented.
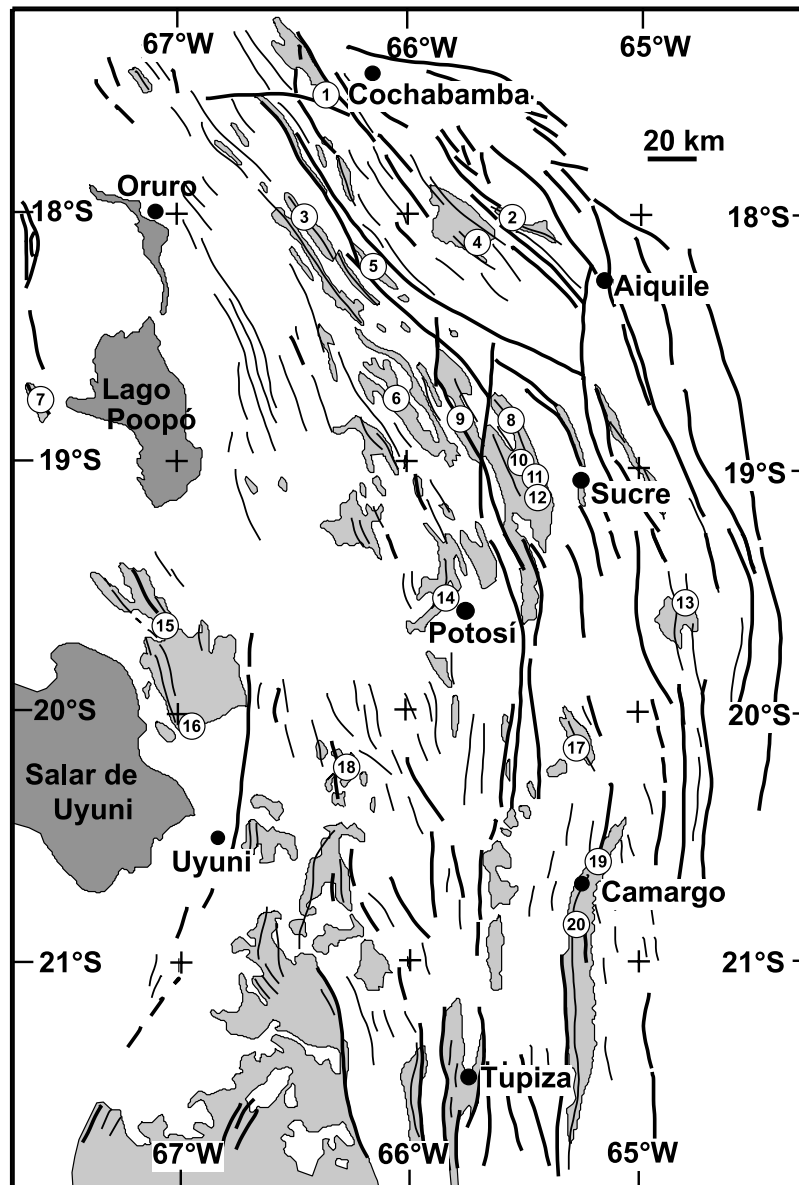
Figure 2. Map of paleomagnetic sampling locations. Numbers indicate sampled sections referred to in text and in Table 1. Trends of major faults and folds are illustrated.

[11] Locality-mean directions were calculated by applying *Fisher* [1953] statistics to the set of normal-polarity site-mean directions and antipodes of reversed-polarity site-mean directions from each locality (discarding site means more than two angular standard deviations from the preliminary mean). The expected direction at a paleomagnetic locality was calculated using the appropriate age reference paleo-magnetic pole for South America from *Besse and Courtillot* [2002]. Concordance/discordance calculations follow the methods of *Beck* [1980] and *Demarest* [1983]. The effects of using reference poles from alternative versions of the Mesozoic-Cenozoic apparent polar wander path for South America are minimal. For example, vertical-axis rotations computed for 70 and 80 Ma units are 2.1° lower if the 70–80 Ma stillstand pole of *Beck* [1999] is used rather than the poles from *Besse and Courtillot* [2002]. If the 60 Ma reference pole of *Roperch and Carlier* [1992] is used rather

than the 60 Ma pole from *Besse and Courtillot* [2002], the computed rotations for the Santa Lucía Formation are decreased by 1.7°. So compared with other uncertainties in determining vertical-axis rotations, those associated with choice of reference paleomagnetic pole are minor.

3. Paleomagnetic Results

[12] Paleomagnetic results are tabulated and described proceeding from north to south across the region of collections (Table A1, auxiliary material[1]). Subdirectories in the ftp site are arranged by journal and paper number. Information on searching and submitting auxiliary materials is found at http:/www.agu.org/pus/esupp_about.html, and
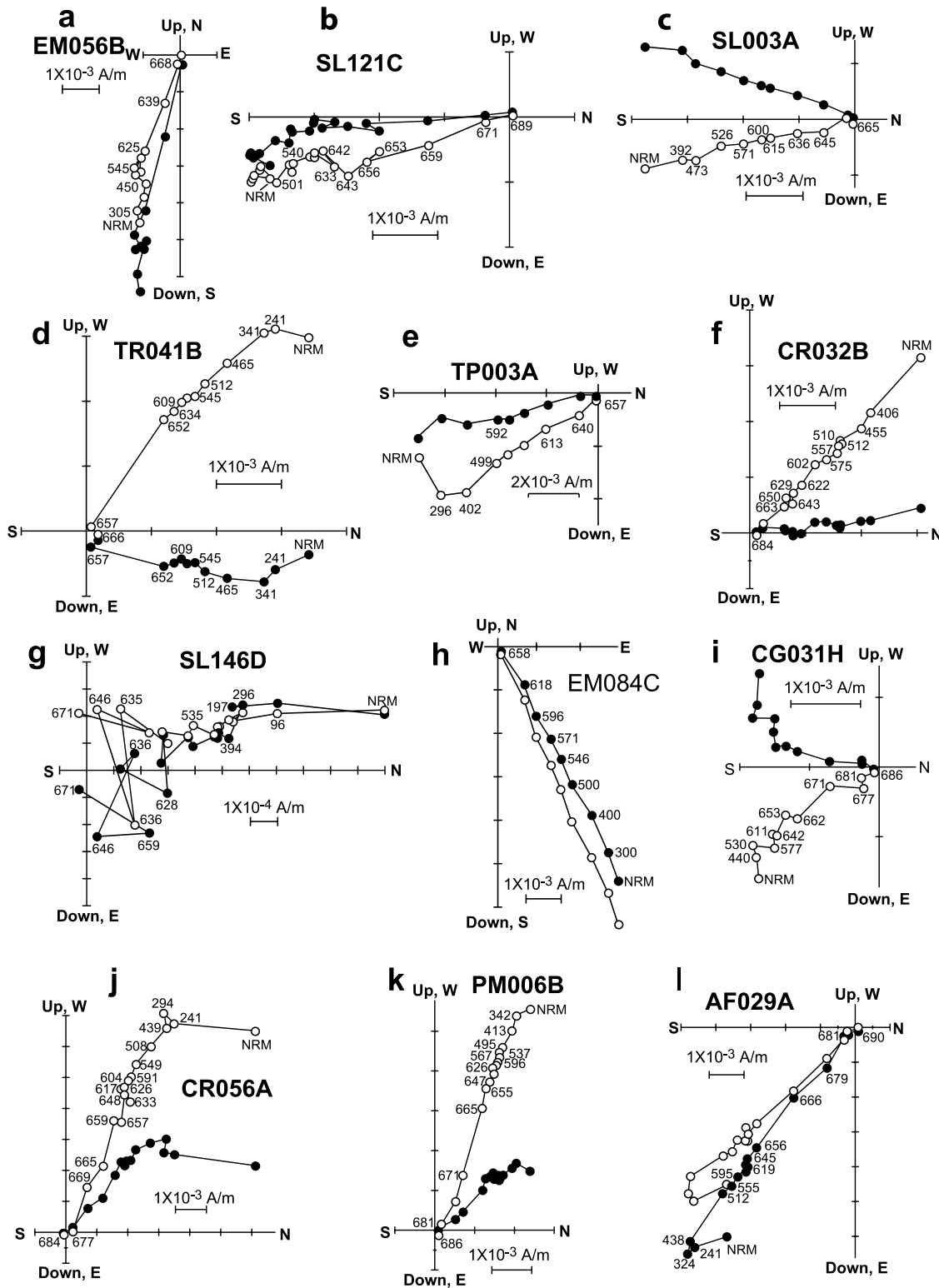

Figure 3. Vector end-point diagrams of typical samples from different sections in stratigraphic (tilt-corrected) coordinates. Filled circles are projections on the horizontal plane and open symbols are projection on the vertical plane. Numbers adjacent to data points indicate temperature in °C. Samples are from (a) El Molino Formation at La Palca, (b) Santa Lucía Formation at Copacabana, (c) Santa Lucía Formation at La Cabaña, (d) Tarapaya Formation at Macha, (e) Santa Lucía Formation at Tiupampa, (f) Coroma Formation at Tica Tica, (g) Santa Lucía Formation at Copacabana (showing unacceptable demagnetization behavior), (h) Santa Lucía Formation at Sucusuma, (i) Potoco Formation at Camargo, (j) El Molino Formation at Maicoma, (k) Cretaceous red sedimentary strata at Inca Pampa (Pilcomayo), and (l) Aroifilla Formation near Maragua.

Table 1. Locality Mean Paleomagnetic Results From the Bolivian Andes[a]

Locality	Location Lat, °S	Location Long, °E	Map No.	Zone	Dist, km	Age, Ma	N	Observed Direction Im, deg	Observed Direction Dm, deg	Observed Direction α95, deg	Reference Pole Lat, deg N	Reference Pole Long, deg E	Reference Pole A95, deg	Rotation R ± ΔR, deg
Potoco (Camargo) Fm, Camargo	20.8	294.8	20	EC	230	50	11	−38.8	18.8	6.4	80.9	164.4	3.4	26.5 ± 7.2
Santa Lucía Fm, La Cabaña	17.5	293.7	1	EC	−160	60	12	−43.6	3.6	3.4	81.1	190.5	2.9	12.8 ± 4.5
Santa Lucía Fm, Copacabana	18.8	292.5	7	AP	−90	60	17	−31.3	317.6	16.1	81.1	190.5	2.9	−33.1 ± 15.4
Muñani Fm, Laguna Umayo	15.8	289.9		AP	−500	60	13	−24.0	319.2	10.4	81.1	190.5	2.9	−31.6 ± 9.4
Santa Lucía Fm, Tiupampa	18.0	294.3	2	EC	−80	60	6	−38.1	347.2	7.9	81.1	190.5	2.9	−3.6 ± 8.4
Santa Lucía Fm, Maragua	19.1	294.6	12	EC	40	60	15	−39.9	8.6	5.2	81.1	190.5	2.9	17.9 ± 6.0
Santa Lucía Fm, Sucusuma	18.1	294.3	4	EC	−70	60	8	−47.3	324.6	4.7	81.1	190.5	2.9	−26.2 ± 6.1
Santa Lucía Fm, Otavi	20.1	294.8	17	EC	140	60	22	−42.7	350.9	8.0	81.1	190.5	2.9	0.2 ± 9.1
Santa Lucía Fm, Camargo North	20.6	294.8	19	EC	200	60	9	−41.4	14.9	8.0	81.1	190.5	2.9	24.2 ± 8.9
El Molino Fm, Maicoma	19.7	293.0	15	AP	20	70	9	−39.3	349.7	9.3	80.3	204.3	3.2	0.0 ± 10.0
El Molino Fm, La Palca	19.5	294.2	14	EC	70	70	18	−41.2	32.7	4.8	80.3	204.3	3.2	43.0 ± 5.8
El Molino Fm, Chita	20.1	293.1	16	AP	70	70	11	−39.6	337.7	8.7	80.3	204.3	3.2	−12.0 ± 9.5
Chaunaca and Aroifilla fm, Chuño	18.2	293.8	5	EC	−90	80	8	−20.7	343.5	8.5	81.4	206.1	5.9	−7.5 ± 8.8
Coroma Fm, TicaTica	20.2	293.7	18	EC	105	80	16	−26.8	4.1	7.5	81.4	206.1	5.9	13.2 ± 8.4
Ariofilla Fm, Chaunaca	19.0	294.6	11	EC	45	90	9	−25.6	45.3	5.8	82.2	202.1	5.2	53.6 ± 6.8
Tarapaya Fm, Khea Khea	18.0	293.6	3	EC	−115	100	17	−29.8	356.3	2.6	81.7	180.1	6.7	4.5 ± 6.2
Tarapaya Fm, Macha	18.8	294.0	6	EC	−20	100	16	−29.7	4.8	2.9	81.7	180.1	6.7	13.0 ± 6.4
Tarapaya Fm, Khara Khara	18.8	294.3	9	EC	10	100	13	−29.4	339.8	2.4	81.7	180.1	6.7	−12.0 ± 6.2
Tarapaya Fm, Maragua	18.9	294.2	10	EC	10	100	5	−34.4	352.1	12.7	81.7	180.1	6.7	0.3 ± 13.6
Ravelo Fm, Ravelo	18.8	294.5	8	EC	10	180	10	−33.2	350.0	6.2	65.5	95.9	5.6	0.2 ± 8.4
Ipaguazú Fm, Pilcomayo	19.5	295.2	13	EC	110	230	12	−38.1	358.5	6.6	77.9	57.8	10.4	9.8 ± 11.4

[a]Locality, geologic formation and location of paleomagnetic sampling; Location Lat and Long, latitude and longitude of sampling locality; Map #, number labeling sampling locality on Figure 2; Zone, labels for localities within the Eastern Cordillera (EC) and Altiplano (AP); Dist, distance of the sampling locality from the axis of curvature of the Bolivian Andes; positive (negative) distances are south (north) of the axis; N, number of paleomagnetic sites at the sampling locality; Observed Direction, locality mean paleomagnetic direction; Im, inclination; Dm, declination; locality mean paleomagnetic direction; α_{95}, radius of 95% confidence limit; Reference Pole Lat and Long, latitude and longitude of reference paleomagnetic pole for South America; A_{95}, 95% confidence limit; Rotation, vertical-axis rotation indicated by difference between observed and expected declination; R, vertical-axis rotation; ΔR, 95% confidence limit for R.

Figure 2). Results from the Muñani Formation at Laguna Umayo (15°45′S; 70°9′W) are tabulated and described by *Sigé et al.* [2004]. Forty-two sites were collected at this locality for magnetostratigraphic analysis. Thirteen site-mean directions from Laguna Umayo pass the selection criteria and all are of reverse polarity. The locality-mean direction is included in Table 1. Comparison with the expected direction determined from the 60 Ma paleomagnetic pole for South America indicates a large counterclockwise rotation $R \pm \Delta R = -31.6° \pm 9.4°$ (Table 1).

3.1. La Cabaña

[13] Twelve sites were collected from the Paleocene Santa Lucía Formation at La Cabaña (17°30′S, 66°20′W). All 12 sites yielded acceptable site-mean ChRM directions from this location labeled #1 in Figure 2. All site-mean directions are of reverse polarity (Table A1, auxiliary material). The paleomagnetic directions in geographic and stratigraphic (tilt corrected) coordinates are illustrated in Figure 4a. Comparison with the 60 Ma expected direction at La Cabaña indicates clockwise rotation $R \pm \Delta R = 12.8° \pm 4.5°$ (Table 1). It is important to note that local dip of strata at this locality exceeds 40° with attendant concern regarding uncertainty of plunge.

3.2. Tiupampa

[14] At Tiupampa (18°0′S; 65°30′W; location #2 of Figure 2), paleomagnetic samples were collected at 17 sites in the Santa Lucía Formation, with six yielding acceptable site-mean ChRM directions [*Butler et al.*, 1995] (Table A1, auxiliary material). All site-mean directions are of reverse polarity. An insignificant rotation ($R \pm \Delta R = -3.6° \pm 8.4°$) results from comparison with the 60 Ma expected direction (Table 1).

3.3. Khea Khea

[15] Eighteen sites from the Albian Tarapaya Formation were collected at Khea Khea (18°1′S; 66°26′W; location #3 of Figure 2) and all but one site yielding acceptable site-mean ChRM directions (Table A1, auxiliary material). All site-mean directions are normal polarity (Figure 4b). An insignificant rotation ($R \pm \Delta R = 4.5° \pm 6.2°$) results from comparison with the 100 Ma expected direction (Table 1). We speculate that the small dispersion of site-mean ChRM directions is due to averaging of geomagnetic secular variation over 10^3 to 10^4 year intervals of post-depositional oxidation during which a chemical remanent magnetization was acquired.

3.4. Sucusuma

[16] At Sucusuma (18°5′S; 65°45′W), 28 sites were collected from the Late Cretaceous to Early Paleocene El Molino Formation and the Paleocene Santa Lucía Formation [*Butler et al.*, 1995]. Eight sites from the Santa Lucía Formation yielded acceptable site-mean ChRM directions from this location (#4 in Figure 2). All site-mean directions are of reverse polarity (Table A1, auxiliary material). Comparison with the 60 Ma expected direction at Sucusuma indicates a counterclockwise rotation $R \pm \Delta R = -26.2° \pm 6.1°$ (Table 1).

3.5. Chuño Ridge

[17] Fourteen sites were collected from the Latest Turonian to Coniacian age Aroifilla Formation and the Santonian to Campanian Chaunaca Formation at Chuño Ridge (18°9′S; 66°13′W; location #5 of Figure 2). Eight sites yielding acceptable site-mean ChRM directions equally divided between normal and reverse polarity (Figure 4c; Table A1, auxiliary material). The reservals test of *McFadden and McElhinny* [1990] is positive with Class C result. The reversed polarity sites are within a stratigraphic package defining a reversed polarity zone that may correlate with Chron C33r of the geomagnetic polarity timescale [*Cande and Kent*, 1992, 1995]. An insignificant rotation ($R \pm \Delta R = -7.5° \pm 8.8°$) results from comparison of the locality-mean direction with the 80 Ma expected direction (Table 1). Local dips of strata at this locality are very large with resultant concern about uncertainty in plunge of structures.

3.6. Macha

[18] Sixteen sites from the Albian Tarapaya Formation were collected at Macha (18°46′S; 66°1′W; location #6 of Figure 2) and all yield acceptable site-mean ChRM directions (Table A1, auxiliary material). All site-mean directions are normal polarity (Figure 5a). As with results from the Tarapaya Formation at Khea Khea, the site-mean directions are tightly clustered ($k > 160$) probably because of time integration of geomagnetic secular variation during post-depositional acquisition of a chemical remanent magnetization. A clockwise rotation ($R \pm \Delta R = 13.0° \pm 6.4°$) results from comparison with the 100 Ma expected direction (Table 1).

3.7. Copacabana

[19] At Copacabana in the central Altiplano (18°46′S; 67°33′W), 27 sites were collected from the Paleocene Upper Member of the El Molino Formation and Santa Lucía Formation. Seventeen sites yielded acceptable site-mean ChRM directions from this location (#7 in Figure 2). Twelve site-mean directions are normal polarity and five are reverse polarity (Table A1, auxiliary material; Figure 5b) but the reversals test is indeterminate. Comparison with the 60 Ma expected direction at Copacabana indicates a counterclockwise rotation $R \pm \Delta R = -33.1° \pm 15.4°$ (Table 1). The observation that site-mean declinations are more dispersed than the inclinations probably indicates differential vertical-axis rotation within the sampled section.

3.8. Ravelo

[20] Eighteen sites from the Jurassic Ravelo Formation were collected at Ravelo (18°49′S; 65°32′W; location #8 of Figure 2) and 10 sites yield acceptable site-mean ChRM directions (Table A1, auxiliary material). All site-mean directions are normal polarity (Figure 5c). An insignificant rotation ($R \pm \Delta R = 0.2° \pm 8.4°$) results from comparison of the locality-mean direction with the 180 Ma expected direction (Table 1). It is noteworthy that the Ravelo Formation yields only normal polarity ChRM directions even though the Middle-Late Jurassic polarity history contains many geomagnetic reversals. We also note that the observed direction has a discordant inclination ($F \pm \Delta F = -27.5° \pm 6.3°$). These unexpected features of the magnetization of the Ravelo Formation are discussed below.

3.9. Khara Khara

[21] Thirteen sites from the Albian Tarapaya Formation were collected at Khara Khara (18°49′S; 65°45′W;
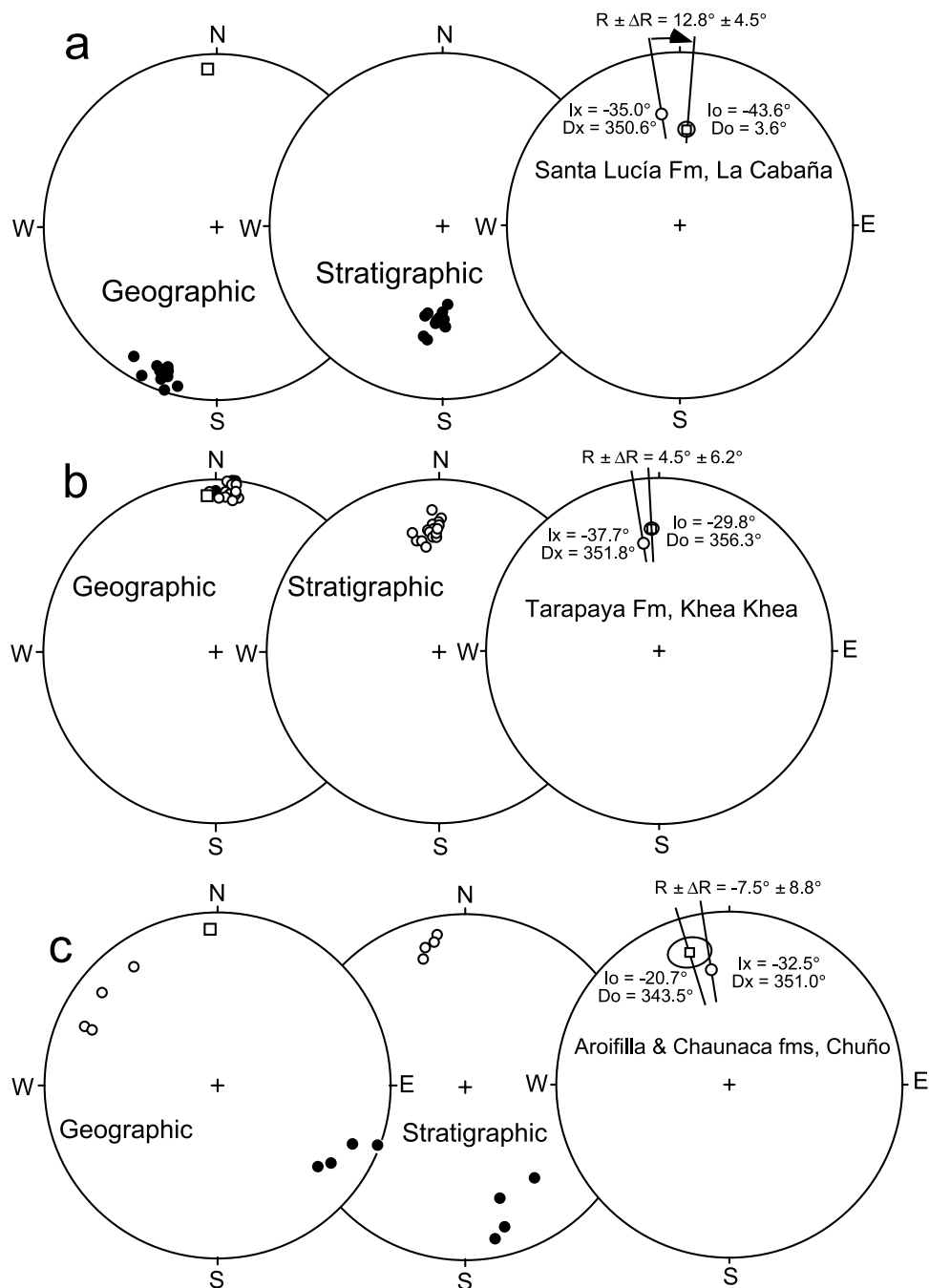
Figure 4. Equal-area projections of site-mean ChRM directions in geographic and stratigraphic (tilt-corrected) coordinates. Filled circles are in lower hemisphere while open circles are in upper hemisphere. Open square in geographic coordinates projection is the present geomagnetic field at the sampling location. Observed locality-mean direction in normal-polarity format is shown by square in projection at right with surrounding 95% confidence limits. Expected direction is indicated by circle in projection at right. Vertical-axis rotation indicated by difference between observed and expected directions and 95% confidence limits ($R \pm \Delta R$) is indicated on projection at right. (a) Santa Lucía Formation at La Cabaña; (b) Tarapaya Formation at Khea Khea; (c) Aroifilla and Chaunaca formations at Chuño.

location #9 of Figure 2) and all produced acceptable site-mean ChRM directions (Table A1, auxiliary material) of normal polarity (Figure 6a). Typical of results from the Tarapaya Formation, the site-mean directions are tightly clustered ($k > 290$ in stratigraphic coordinates). A counter-clockwise rotation ($R \pm \Delta R = -12.0° \pm 6.2°$) results from comparison with the 100 Ma expected direction (Table 1).

Local dips of strata at this locality are moderate with some concern about uncertainty in plunge.

3.10. Maragua

[22] Six sites were collected from the Tarapaya Formation at a locality near Maragua (18°56′S; 65°49′W; location #10 of Figure 2) with five yielding acceptable
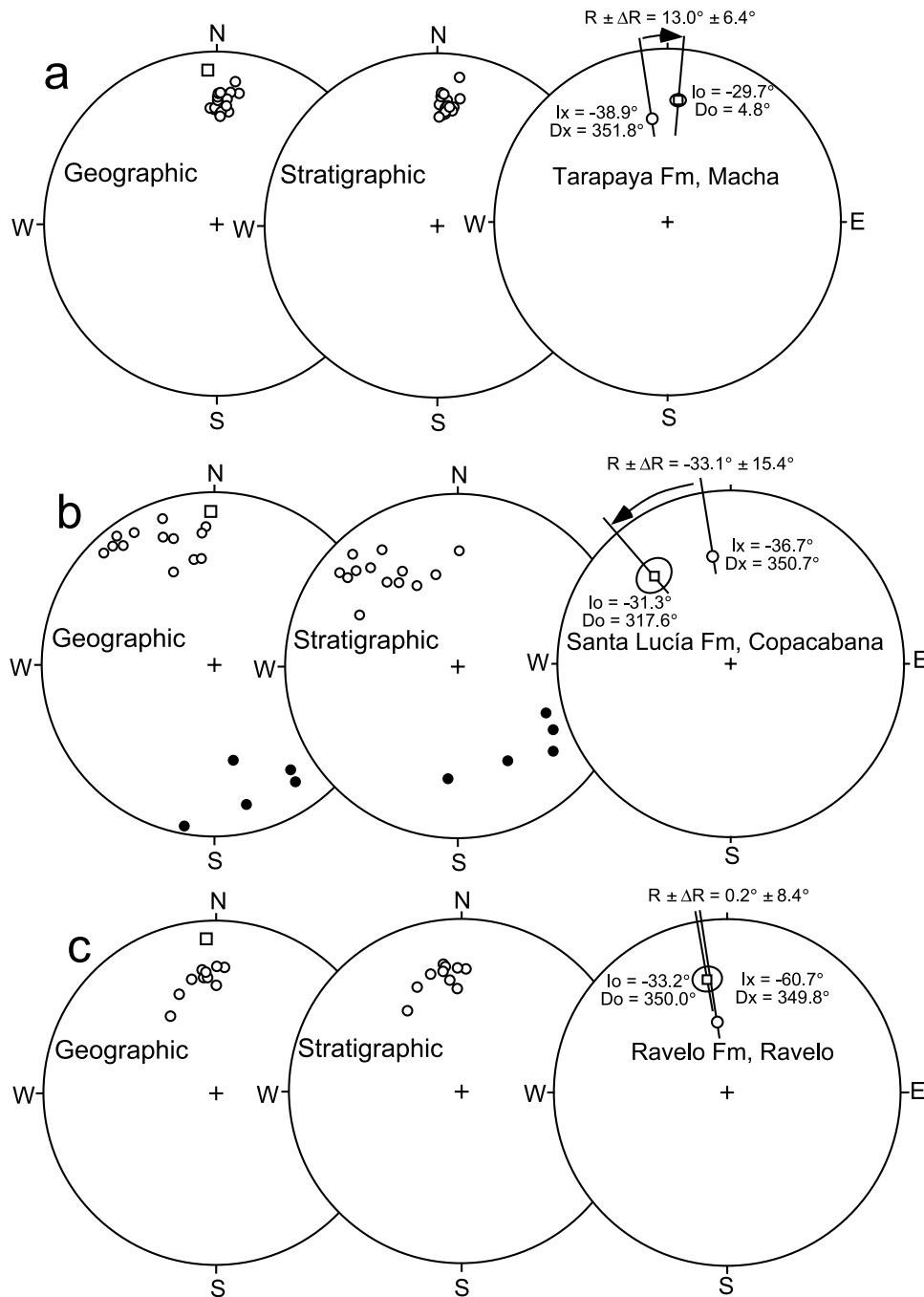
Figure 5. Site-mean directions, observed locality-mean direction, and vertical-axis rotation for (a) Tarapaya Formation at Macha, (b) Santa Lucía Formation at Copacabana, and (c) Ravelo Formation at Ravelo. Symbols as in Figure 4.

normal polarity site-mean ChRM directions (Table A1, auxiliary material; Figure 6b). An insignificant rotation ($R \pm \Delta R = 0.3° \pm 13.6°$) results from comparison of the locality-mean direction with the 100 Ma expected direction (Table 1). At a nearby locality, 16 sites were collected from the Aroifilla Formation (18°59′S; 65°26′W; location #11 of Figure 2). Nine sites yielded acceptable site-mean ChRM directions from this location (Table A1, auxiliary material; Figure 6c). The three normal polarity and six reverse polarity site-mean directions pass the reversals test with Class C. If these directions are

primary, a large clockwise rotation ($R \pm \Delta R = 53.6° \pm 6.8°$) results from comparison of the locality-mean direction with the 90 Ma expected direction (Table 1). However, the Latest Turonian to Coniacian age of the Aroifilla Formation indicates that only normal polarity ChRM directions should be observed. As discussed below, the primary nature of the magnetization from the Mesozoic formations at several locations in the Eastern Cordillera is questionable.

[23] Fifteen sites were collected from strata of the Santa Lucía Formation (and possibly the overlying Cayara For-
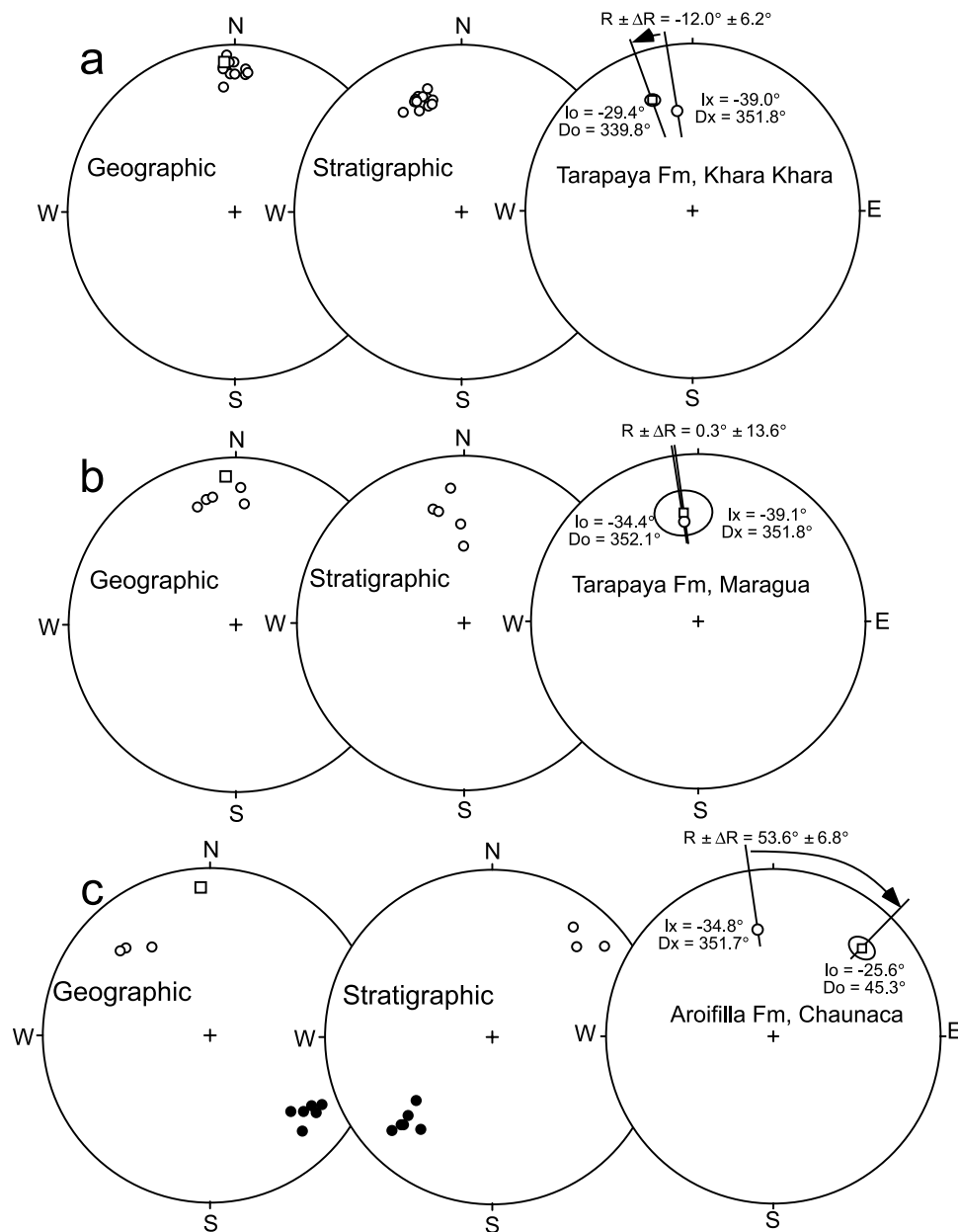
Figure 6. Site-mean directions, observed locality-mean direction, and vertical-axis rotation for (a) Tarapaya Formation at Khara Khara, (b) Tarapaya Formation at Maragua, and (c) Aroifilla Formation at Chaunaca. Symbols as in Figure 4.

mation?) exposed within the Maragua syncline (19°3′S; 65°26′W; location #12 of Figure 2). All sites yielded acceptable site-mean ChRM directions, and the 13 normal and two reverse polarity sites pass the reversals test with Class C (Table A1, auxiliary material; Figure 7a). Variations in bedding attitude are sufficient to provide a positive fold test of paleomagnetic stability at the 95% confidence level. Magnetostratigraphic and paleontologic studies of the Santa Lucía Formation [*Sempere et al.*, 1997] have indicated that the entire formation was deposited during Chron C26r. Thus the dominance of normal polarity in the strata exposed within the Maragua syncline is puzzling. This could indicate that the sampled section includes strata of the Cayara Formation or that the Santa Lucía Formation is time

transgressive. These uncertainties have negligible effect on vertical-axis rotations calculated from the locality-mean paleomagnetic direction. Comparison with the 60 Ma expected direction at Maragua indicates clockwise rotation $R \pm \Delta R = 17.9° \pm 6.0°$ (Table 1).

3.11. Pilcomayo

[24] At Pilcomayo (locality #13 of Figure 2), 15 sites were collected from the Early to Middle Triassic Ipaguazú Formation at Incapampa Syncline (19°27′S; 64°50′W). Eight sites provided acceptable normal polarity site-mean ChRM directions and four produced reverse polarity site-mean directions (Figure 7b; Table A1, auxiliary material). The reversals test of *McFadden and McElhinny* [1990] is
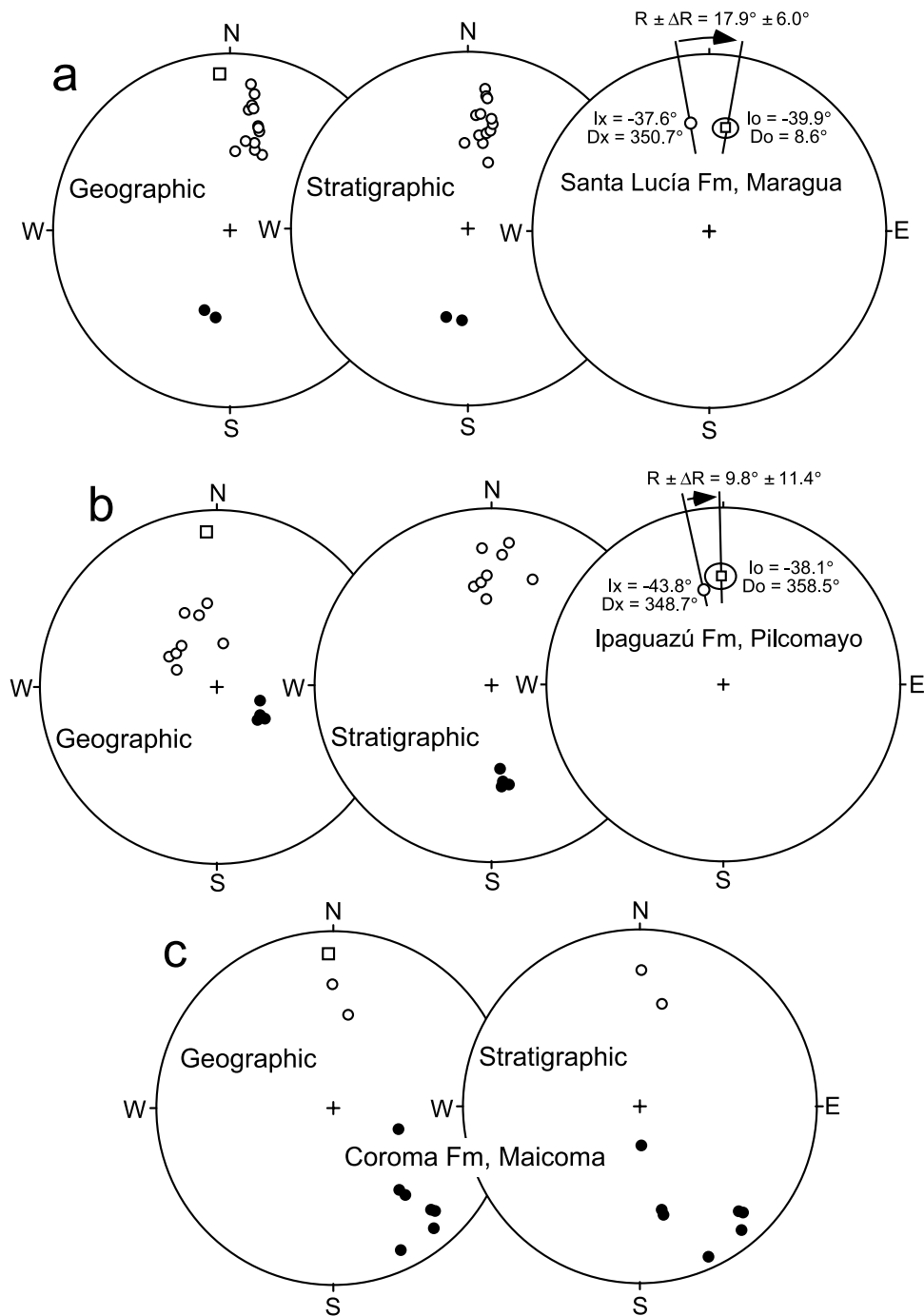
Figure 7. Site-mean directions, observed locality-mean direction, and vertical-axis rotation for (a) Santa Lucía Formation at Maragua, (b) Ipaguazú Formation at Pilcomayo (Incapampa syncline), and (c) Coroma Formation at Maicoma. Symbols as in Figure 4.

negative because the critical angle is 10.1° while the observed angle between the mean of normal polarity sites and the antipode of reversed polarity sites is 11.9°. However, this negative reversals test is primarily the result of very tight grouping of reverse polarity site-mean directions (k = 344) that probably indicates insufficient averaging of geomagnetic secular variation by these four sites. While the locality-mean direction is less robust than desired, the insignificant rotation (R ± ΔR = 9.8° ± 11.4°) indicated by comparison of this direction with the 230 Ma expected

direction is an important result from this isolated area (Table 1).

3.12. La Palca

[25] At La Palca (19°32′S; 65°50′W; locality #14 of Figure 2), 62 sites were collected from a 480-m-thick section of Late Cretaceous to Early Paleocene El Molino Formation exposed in the Miraflores Syncline [*Butler et al.*, 1995]. Eighteen sites yielded acceptable site-mean ChRM directions with five normal polarity and 13 reversed polarity
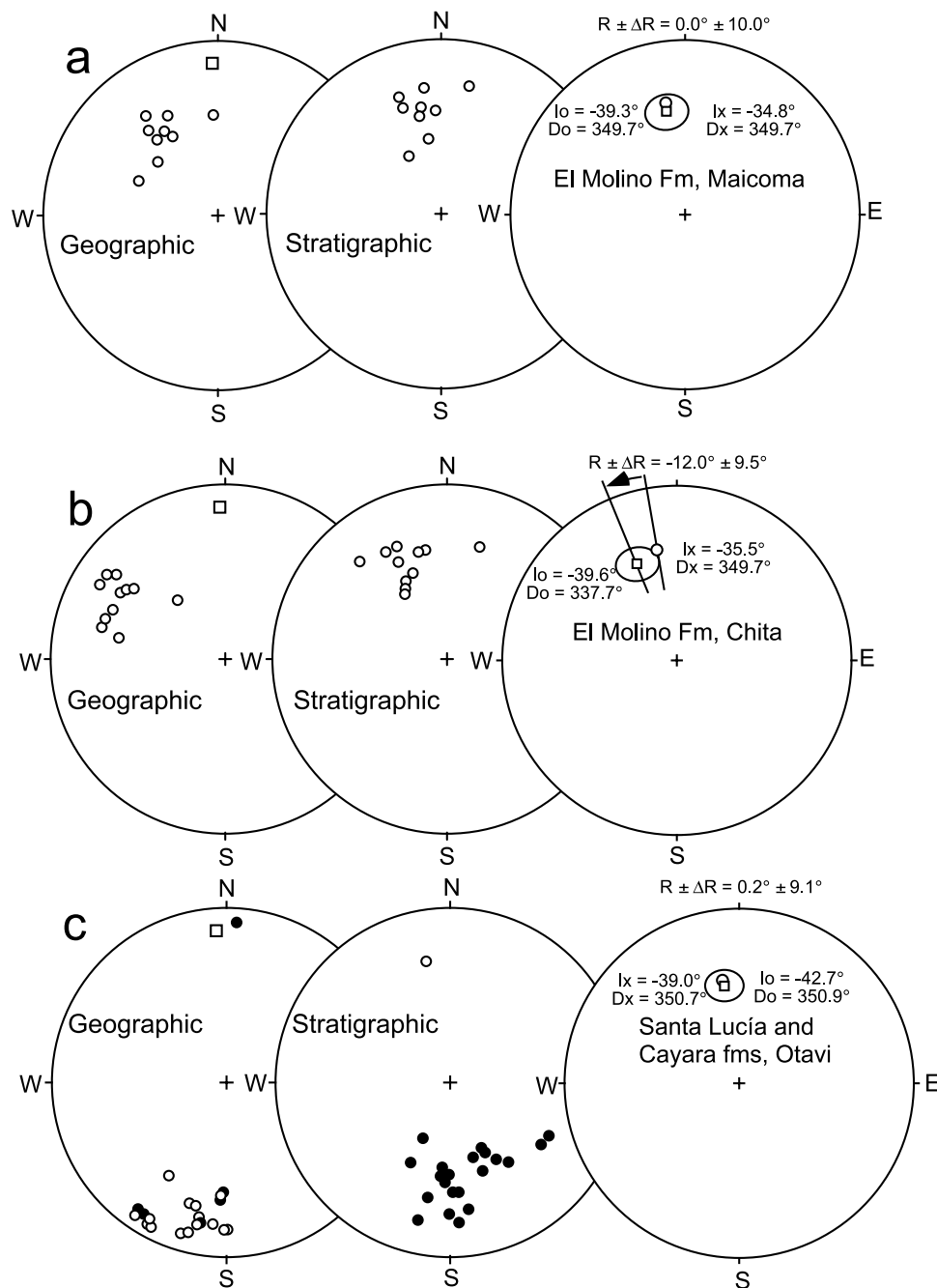
Figure 8. Site-mean directions, observed locality-mean direction, and vertical-axis rotation for (a) El Molino Formation at Maicoma, (b) El Molino Formation at Chita, and (c) Santa Lucía Formation at Otavi. Symbols as in Figure 4.

directions passing the reversals test with C classification (Table A1, auxiliary material). Comparison with the 70 Ma expected direction at La Palca indicates a large clockwise rotation $R \pm \Delta R = 43.0° \pm 5.8°$ (Table 1).

3.13. Maicoma

[26] Twenty-three sites were collected from the Campanian Coroma Formation at a locality near Maicoma (19°40′S; 67°3′W; location #15 of Figure 2). Seven acceptable reverse polarity site-mean directions and two normal polarity directions were observed (Table A1, auxiliary material; Figure 7c). These directions fail the reversals test with an observed 29.8° angle between the mean of normal polarity sites and the antipode of reversed polarity sites. The site-mean directions are poorly grouped ($k = 9.4$ in stratigraphic coordinates) and we do not regard these data as reliable for determination of vertical-axis rotation. Higher quality results were obtained from the Middle Member of the El Molino Formation in this area (19°41′S; 67°3′W; location #15 of Figure 2). From 13 sites collected, nine yielded acceptable normal polarity site-mean ChRM directions (Table A1, auxiliary material; Figure 8a). Comparison

with the 70 Ma expected direction at Maicoma indicates no rotation ($R \pm \Delta R = 0.0° \pm 10.0°$; Table 1).

3.14. Chita

[27] Thirteen sites were collected from the Middle Member of El Molino Formation at Chita (20°5′S; 66°53′W; location #16 of Figure 2). Eleven normal polarity site-mean directions passed the acceptability criteria. Comparison with the 70 Ma expected direction at Chita indicates a counterclockwise rotation $R \pm \Delta R = -12.0° \pm 9.5°$ (Figure 8b; Table 1). Local dips of strata at this locality exceed 40° with attendant uncertainty in plunge and resulting uncertainty in derived vertical-axis rotation.

3.15. Otavi

[28] Twenty-nine sites were collected from strata of the Santa Lucía Formation and the overlying Cayara Formation in the center of the Otavi syncline (20°6′S; 65°14′W; location #17 of Figure 2). One acceptable normal polarity and 21 reverse polarity site-mean directions were observed (Table A1, auxiliary material; Figure 8c). With only a single normal polarity direction, the reversals test is indeterminate. Comparison with the 60 Ma expected direction at Otavi indicates no rotation ($R \pm \Delta R = 0.2° \pm 9.1°$; Table 1). Local dips of strata at this locality are very large (locally overturned) with attendant concern about plunge of structures and the derived vertical-axis rotation.

3.16. Tica Tica

[29] At Tica Tica (20°11′S; 66°19′W; locality #18 of Figure 2), 21 sites were collected from the Coroma Formation. Sixteen sites yielded acceptable normal polarity site-mean ChRM directions (Table A1, auxiliary material; Figure 9a). Comparison with the 80 Ma expected direction indicates a significant clockwise rotation $R \pm \Delta R = 13.2° \pm 8.4°$ (Table 1).

3.17. Camargo

[30] A few kilometers north of Camargo (20°36′S; 65°10′W; locality #19 of Figure 2), 14 sites were collected from the El Molino and Santa Lucía formations. Seven acceptable normal polarity and two reversed polarity site-mean ChRM directions were observed (Table A1, auxiliary material; Figure 9b). These directions pass the reversals test with C classification [*McFadden and McElhinny*, 1990]. Comparison with the 60 Ma expected direction at Camargo indicates clockwise rotation $R \pm \Delta R = 24.2° \pm 8.9°$ (Table 1). A few kilometers south of Camargo (20°45′S; 65°14′W; locality #20 of Figure 2), 57 sites were collected from a stratigraphic sequence of the Camargo Formation that on paleontological grounds may correlate with the Potoco Formation (see *Sempere et al.* [1997] and *DeCelles and Horton* [2003] for discussions). Following rejection of one outlier site-mean direction, eight acceptable normal polarity and four reverse polarity site-mean directions pass the reversals test with class C (Table A1, auxiliary material; Figure 9c). Comparison with the 60 Ma expected direction at Camargo indicates a clockwise rotation $R \pm \Delta R = 26.5° \pm 7.2°$ (Table 1).

4. Regional Fold Tests

[31] With the exception of the positive fold test for the Santa Lucía Formation at Maragua, variations in bedding attitude within sampling locations are insufficient to yield definitive local fold tests. The relative timing of magnetization and folding must be assessed through regional fold tests. Because variations in locality-mean declinations are clearly evident in the data, the most effective field test of stability of the characteristic magnetization is the inclination-only fold test. The inclination-only statistical methods described by *Watson and Enkin* [1993] and *Enkin and Watson* [1996] were used.

[32] Block-rotation Fisher analysis is useful for sample collections from several rigid blocks that have undergone differential rotation but are not internally deformed. However, this internally undeformed condition is questionable in the case of outcrops in the Altiplano and Eastern Cordillera of Bolivia. Indeed site-mean directions from within several sampling localities show a spread of declinations suggesting differential vertical-axis rotation within sampled stratigraphic sections, perhaps by slip on bedding planes. Accordingly we did not use the block-rotation version of the inclination-only fold test. As described by *Watson and Enkin* [1993] and *Enkin and Watson* [1996], the parameter-estimation method of performing the inclination-only fold test determines the degree of untilting that produces minimum dispersion of site-mean paleomagnetic inclinations to determine whether the magnetization is pre-tilting, post-tilting, or intermediate. If the optimum unfolding includes 100% but excludes 0% unfolding, the inclination-only fold test is positive.

[33] Figures 10a and 10b illustrate site-mean directions obtained from 82 sites in Tertiary strata of the Altiplano and Eastern Cordillera in geographic and corrected (stratigraphic) coordinates, respectively (Table A1, auxiliary material). Results from Laguna Umayo were excluded from this analysis because of complexities described by *Sigé et al.* [2004]. As is apparent in Figure 10b, the clustering of site-mean inclinations is improved by restoring bedding to horizontal; the best estimate of precision parameter, k, increases from 5.0 in geographic coordinates to 30.2 in corrected coordinates. Illustrated in Figure 10c is k as a function of percent unfolding. Optimum unfolding occurs at 97.1% with 95% confidence limits of 89.9% and 104.0% unfolding. Thus site-mean directions from these Tertiary strata pass the inclination-only fold test consistent with a primary origin for the characteristic remanent magnetization acquired when bedding was horizontal.

[34] Paleomagnetic directions reported herein from 133 sites in Mesozoic rocks are illustrated in Figures 10d and 10e in geographic and corrected (stratigraphic) coordinates, respectively (Table A1, auxiliary material). The best estimate of the precision parameter, k, increases from 12.4 in geographic coordinates to 32.0 in stratigraphic coordinates and is plotted as function of percent unfolding in Figure 10f. There is a broad maximum in k value between 80% and 100% unfolding. Simulation indicates optimum unfolding at 89.2%, with 95% confidence limits of 86.4% and 92.2% unfolding. The optimum percent unfolding is thus distinct from 100% and these Mesozoic data fail the inclination-only fold test. (Site-mean directions from the Tarapaya Formation at KharaKhara, Maragua, Macha, and KheaKhea are near the present geomagnetic field direction in geographic coordinates and could therefore be affected by recent remagnetization. The inclination-only analysis
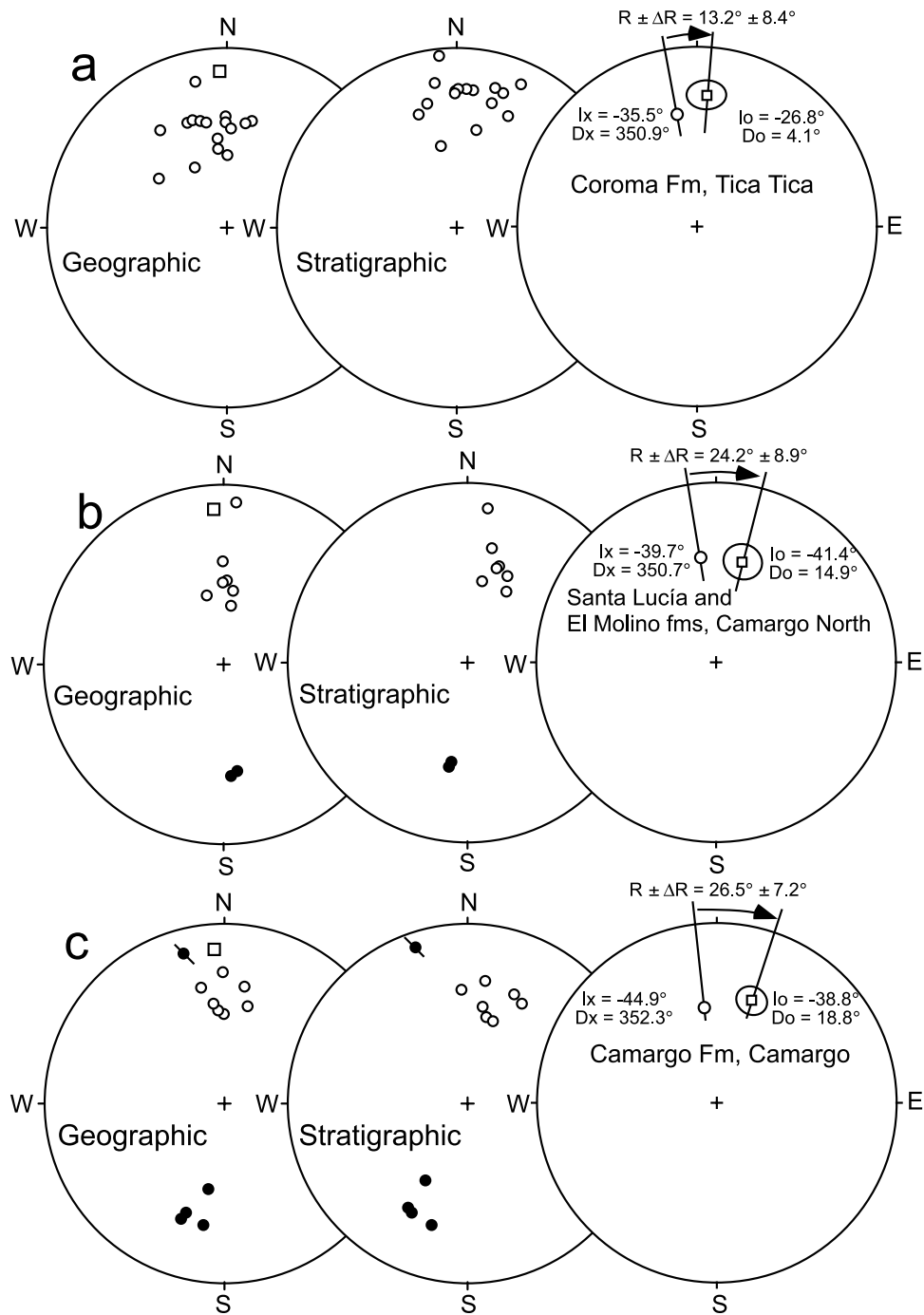
Figure 9. Site-mean directions, observed locality-mean direction, and vertical-axis rotation for (a) Coroma Formation at Tica Tica; (b) Santa Lucía Formation north of Camargo; and (c) Potoco Formation south of Camargo. Symbols as in Figure 4.

was applied to the remaining 82 sites following deletion of these Tarapaya Formation sites. Simulation indicated optimum unfolding at 76.9%, with 95% confidence limits of 72.7% and 80.4% unfolding. This indicates that failure of the inclination-only fold test is not due to a present-field overprint of the Tarapaya Formation.) It is unclear what inference should be drawn from the observation that optimum unfolding is statistically distinct from 100% unfolding. We doubt this indicates synfolding secondary remagnetization for Mesozoic strata over the broad sam-

pling region in the Eastern Cordillera and Altiplano but local remagnetization of Mesozoic units at some locations during Andean deformation is a possibility. In the above presentations of paleomagnetic data from Mesozoic strata, we noted several inconsistencies between ages of Mesozoic strata sampled and paleomagnetic polarity observed. The discordant inclination from the Ravelo Formation could also indicate an age of magnetization much younger than the Jurassic age of the sampled rocks (Figure 5c). As demonstrated by paleomagnetic results from red sedimentary strata
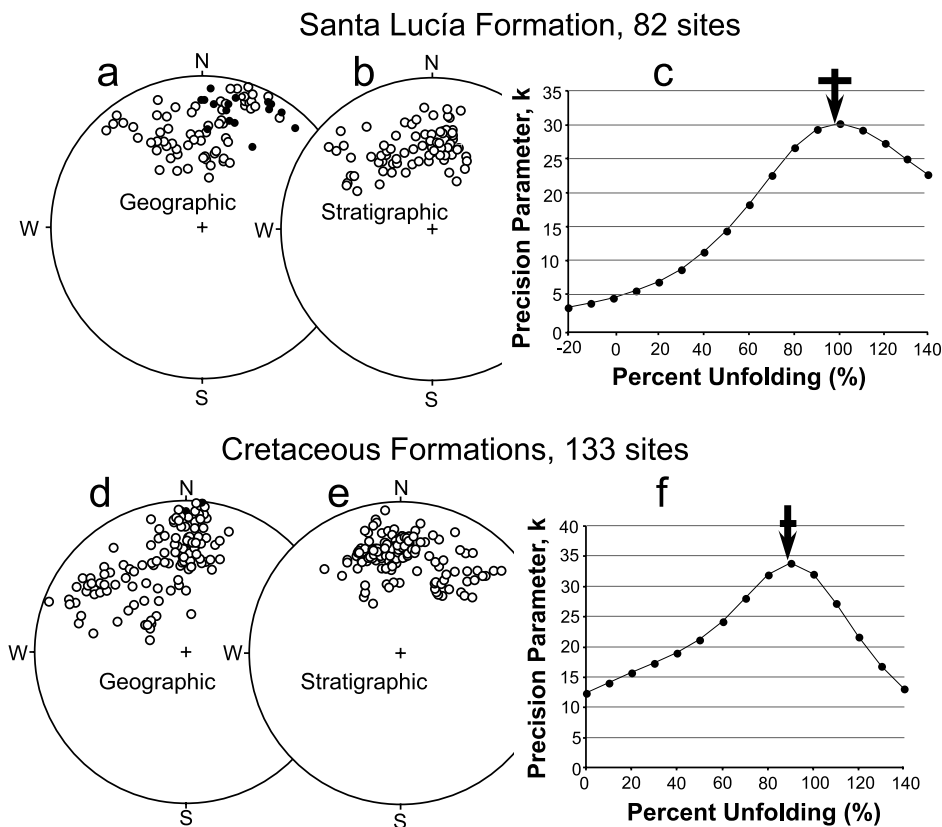
Figure 10. Site-mean directions and inclination-only statistical parameters. Equal-area projections of 82 site-mean ChRM directions from the Santa Lucía Formation are shown in geographic and stratigraphic (tilt-corrected) coordinates in (a) and (b), respectively. Best estimate of precision parameter, k, from inclination-only statistical analysis is plotted as a function of percent unfolding in (c). Equal-area projections of 133 site-mean ChRM directions from Mesozoic units are shown in geographic and stratigraphic (tilt-corrected) coordinates in (d) and (e), respectively. Arrows in (c) and (f) indicate optimum unfolding determined from parametric simulation. Horizontal lines through arrows indicate the 95% confidence limits on optimum unfolding. See text for discussion.

of the Devonian Vila Vila Formation at Pongo in the Eastern Cordillera, Tertiary remagnetization of older strata has occurred during Andean deformation at some locations [*Libarkin et al.*, 1998]. Taken together with results from the inclination-only fold test, these problems indicate that the primary origin of magnetization for Mesozoic strata at a number of locations is in doubt. Accordingly vertical-axis tectonic rotations interpreted from paleomagnetism of Mesozoic units of the Altiplano and Eastern Cordillera is much less certain than are rotations determined from paleomagnetic data of Tertiary formations. Accordingly, we place less emphasis on geologic interpretation of results from Mesozoic strata than results from Cenozoic strata.

[35] Vertical-axis rotations calculated from paleomagnetic results presented in this paper are listed in Table 1 and illustrated in Figure 11. Rotations determined from Mesozoic rocks and from localities with ≤8 sites are less reliable than rotations calculated from paleomagnetic directions based on >8 sites in Tertiary strata. The more reliable rotations are displayed with bold arrows in Figure 11. The region displayed in the map of Figure 11 includes the axis of curvature of the Bolivian Orocline. To first order, the pattern noted by *Isacks* [1988] of clockwise (positive)

rotations south of the axis and counterclockwise (negative) rotations north of the axis is evident in Figure 11, although with several important exceptions. The pattern of vertical-axis rotations is more completely investigated below following compilation of published paleomagnetic data and consideration of geologic constraints for analysis of rotations in the central Andes.

5. Discussion and Conclusions

[36] Paleomagnetic data from a number of locations within the Bolivian Orocline were recently published by *Lamb* [2001a]. Although based on small numbers of samples, *Lamb* [2001a] selected structural settings of samples that could sometimes provide local fold tests of paleomagnetic stability. The selection of sampling localities in the present study favored thick sections of red sedimentary strata in the central parts of major folds where large numbers of samples were collected. As documented above, the resulting paleomagnetic data provide robust determinations of vertical-axis rotation for most sampled sections but with the liability that local fold tests are rarely available and paleomagnetic stability must be assessed using a
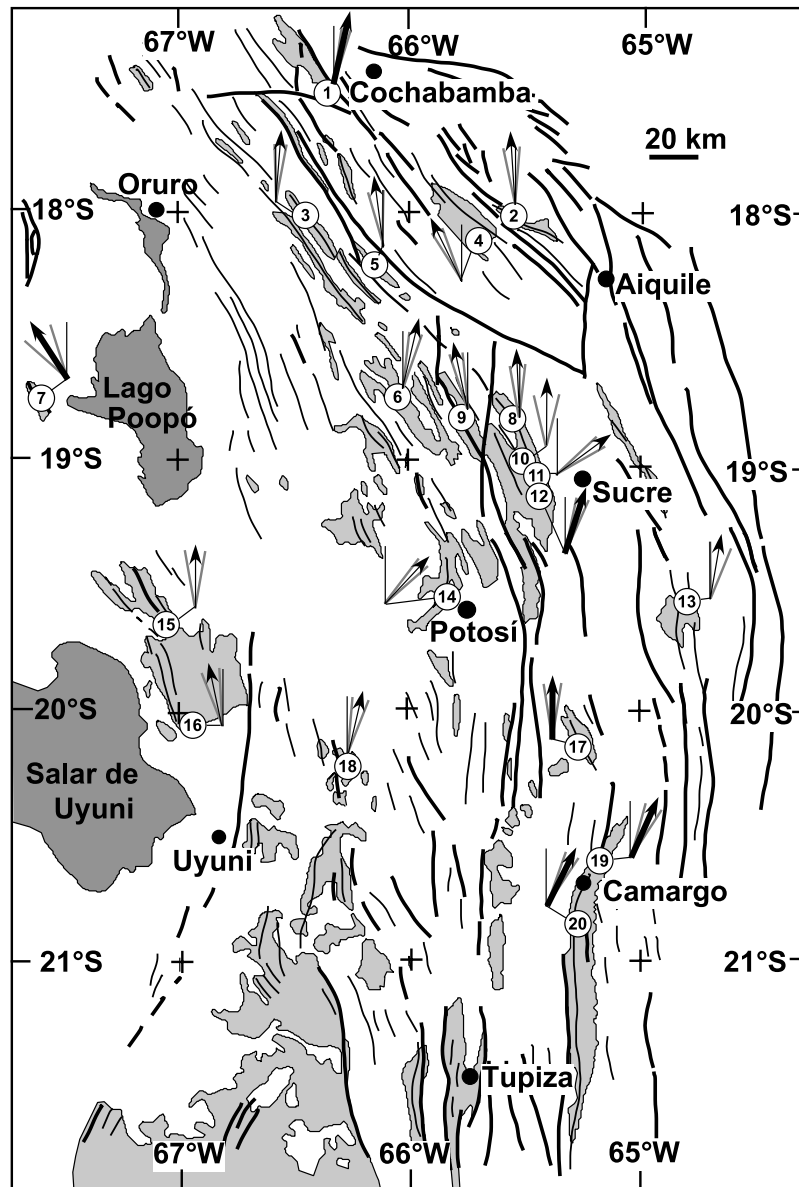
Figure 11. Map of vertical-axis rotations. Rotations ($R \pm \Delta R$) are shown by deflection of arrow from north indicated by thin black line. Confidence limits (95%) on vertical-axis rotation are indicated by gray lines on either side of the arrow. Vertical-axis rotations determined by >8 site-mean paleomagnetic directions from Cenozoic strata are shown by bold arrows and are considered more robust than determinations based on fewer sites or on paleomagnetic directions from Mesozoic strata. See text for discussion.

regional inclination-only fold test. The resulting determinations of vertical-axis rotation by *Lamb* [2001a] are in general agreement with those presented here. At Otavi for example, *Lamb* [2001a] determined $R \pm \Delta R = -0.3° \pm 18.2°$ from 12 samples of El Molino Formation limestone. On the basis of results from 162 paleomagnetic samples at 22 sites in the Santa Lucía Formation and Cayara Formation at Otavi, we determined a vertical-axis rotation $R \pm \Delta R = 0.2° \pm 9.1°$ (Table 1). Immediately north of Camargo, *Lamb* [2001a] determined $R \pm \Delta R = 18.6° \pm 17.7°$ based on 21 samples from the Santa Lucía Formation. Our results from 59 samples from 9 sites at this location indicate $R \pm \Delta R = 24.2° \pm 8.9°$. At other common sampling localities,

significant differences in calculated vertical-axis rotation are evident. At Chita, *Lamb* [2001a] determined $R \pm \Delta R = 7° \pm 6°$ using six samples from the El Molino Formation whereas our results from 11 sites (74 samples) yield $R \pm \Delta R = -12.0° \pm 9.5°$. However, it is noteworthy that dips of the red bed strata at our Chita locality exceed 40° with resulting uncertainty about effects of plunge on the derived vertical-axis rotation. For common collecting locations, we use our determinations of vertical-axis rotations because of the larger number of samples in the present study.

[37] *Libarkin et al.* [1998] argued that paleomagnetic data from Devonian through Late Permian strata of the Eastern Cordillera and Subandean zone were best grouped at

Table 2. Paleomagnetic Determinations of Vertical-Axis Rotation From Cenozoic Units of the Bolivian Andes[a]

| Locality | Location | | Zone | Dist, km | Age, Ma | N | Observed direction | | | Reference Pole | | | Rotation | Ref |
	Lat, °S	Long, °E					Im, deg	Dm, deg	α95, deg	Lat, °N	Long, °E	A95, deg	R ± ΔR, deg	
Subandean Tertiary	20.6	296.0	SA	270	25	8	−30.9	5.0	6.7	82.8	158.1	3.8	10.4 ± 7.1	1
Micaña	17.5	292.6	EC	−210	10	25	−25.8	355.0	5.9	84.0	154.8	2.7	−0.7 ± 5.7	2
Quebrada Honda	22.0	294.6	EC	340	10	79	−40.7	17.8	3.9	85.4	162.5	2.0	21.6 ± 4.5	2
Cerdas	21.0	294.0	EC	200	20	24	−39.1	10.1	7.0	84.0	154.8	2.7	14.4 ± 7.6	3
Salla	17.2	292.3	EC	−250	20	58	−37.4	353.4	5.4	84.0	154.8	2.7	−2.2 ± 5.9	2
Corque syncline	17.5	291.8	AP	−240	10	79	−22.4	346.6	2.5	84.0	154.8	2.7	−9.0 ± 3.2	4
Quehua	19.9	293.1	AP	60	10	25	−37.9	15.3	9.3	84.0	154.8	2.7	19.7 ± 9.7	3
North Uyuni	20.0	293.0	AP	60	20	10	−41.1	358.4	16.7	84.0	154.8	2.7	2.8 ± 18.1	5
Lipez	21.8	293.5	AP	270	20	16	−38.6	37.5	10.8	84.0	154.8	2.7	41.9 ± 11.4	5
Viacha	16.8	291.5	AP	−330	30	12	−31.6	349.3	10.9	82.8	158.1	3.8	−5.1 ± 10.8	5
Chuquichambi	18.0	292.2	AP	−180	30	13	−27.8	332.4	6.7	82.8	158.1	3.8	−22.0 ± 6.9	5

[a]Locality, location of paleomagnetic sampling; Location Lat and Long, Latitude and longitude of sampling locality; Zone, labels for localities within the Subandean plus Interandean zones (SA), Eastern Cordillera (EC), and Altiplano (AP); Dist, distance of the sampling locality from the axis of curvature of the Bolivian Andes, positive (negative) distances are south (north) of the axis; Age, approximate age in millions of years of rocks sampled; N, number of paleomagnetic sites at the sampling locality; Observed direction, locality mean paleomagnetic direction; Im, Inclination; Dm, Declination; α95, radius of 95% confidence limit; Reference Pole Lat and Long, latitude and longitude for the reference paleomagnetic pole for South America; A95, 95% confidence limit; Rotation, vertical-axis rotation indicated by difference between observed and expected declination; R, vertical-axis rotation; ΔR, 95% confidence limit for R. Ref, reference: 1, *Lamb* [2001a]; 2, *MacFadden et al.* [1990]; 3, *MacFadden et al.* [1995]; 4, *Roperch et al.* [1999]; 5 *Roperch et al.* [2000].

80% unfolding indicating remagnetization during Tertiary folding. While accepting a Tertiary origin for magnetization of the Devonian Vila Vila Formation at Pongo, *Roperch et al.* [2000] reinterpreted the paleomagnetic directions of *Libarkin et al.* [1998] as acquired during the Permo-Carboniferous Reversed-Polarity Superchron. *Roperch et al.* [2000] then used these directions to determine Tertiary vertical-axis rotations of the Subandean zone. Following exclusion of results from one locality of *Libarkin et al.* [1998], *Roperch et al.* [2000] and *Gilder et al.* [2003] correctly observed that maximum clustering of paleomagnetic directions from Paleozoic rocks in the southern Subandean zone occurs at 100% unfolding. This indicates that the Paleozoic strata acquired the characteristic magnetization prior to folding. Ages of the sampled formations are Mississippian and Late Permian, preceding and following the Permo-Carboniferous Reversed-Polarity Superchron. Indeed *Libarkin et al.* [1998] observed normal-polarity magnetization in the Mississippian Tupambi and Taiguati formations. Thus assigning the age of (re)magnetization to the reversed-polarity superchron is at best highly speculative. Additionally there are major uncertainties in determining the Late Carboniferous reference pole either directly from South American paleomagnetic data or by rotating paleomagnetic poles from Gondwana continents into South American coordinates. Because of these uncertainties, determining Neogene vertical-axis rotation of the Subandean zone using the paleomagnetic data reported by *Libarkin et al.* [1998] is unjustified. Fortunately, *Lamb* [2001a] published a critical paleomagnetic determination of vertical-axis rotation from Oligo-Miocene sedimentary strata of the Subandean Zone. This result is included in Table 2 and features in the discussion below.

[38] Most analyses of vertical-axis rotations have examined paleomagnetic data in latitudinal belts across the entire width of the Andes [*Isacks*, 1988]. This is a potentially effective method for deciphering major latitudinal variations. However, it is now reasonably established that the Bolivian Andes have undergone a west-to-east progression of fold-thrust development that was dominantly but not exclusively within the Eastern Cordillera between ∼35 Ma

and ∼10 Ma. From ∼10 Ma to present, thin-skinned deformation occurred mostly within the Subandean and Interandean zones with minor crustal shortening internal to the Altiplano. We thus analyze crustal shortening estimates and attendant vertical-axis rotations in the Bolivian Andes by analyzing these zones that experienced deformation during different time intervals. When analyzing active deformation in the Central Andes determined from GPS networks, *Bevis et al.* [2001] developed a model including an Andean microplate between the Nazca and South American plates. These authors also noted the importance of along-strike variations in convergence between this Andean microplate and interior South America. *Bevis et al.* [2001] specifically noted a decrease in modern shortening rate of the Subandean zone southward from the orocline axis.

[39] If along-strike variations in crustal shortening have occurred systematically during Andean deformation, the amount of shortening along different profiles across the Bolivian Andes can be used to calculate the Euler rotations describing those variations. Although kinematics of fold-thrust belts on continents are intrinsically more complex than motions of oceanic lithospheric plates for which Euler rotation analyses were introduced to geology, useful quantification of vertical-axis rotations within shortened belts can be derived. The utility of Euler pole analysis is that shortening estimates along two or more profiles can be used to determine an ''effective'' Euler rotation that predicts shortening along any profile within that part of the fold-thrust belt. Paleomagnetically determined vertical-axis rotations from that region can then be compared to the computed Euler rotation to determine how well along-strike variations of shortening within the fold-thrust belt account for the observed vertical-axis rotations. We cannot calculate confidence limits on these Euler rotations as is done for rotations of oceanic plates determined from analyses of marine magnetic anomalies because: (1) there are too few shortening estimates to effectively use statistical methods; and (2) individual shortening estimates from balanced cross sections have uncertainties that are difficult to quantify. Nevertheless Euler rotation analysis has not previously been applied to the Bolivian fold-thrust belt and the results

described below demonstrate that along-strike variation of shortening can indeed account for a significant part of the observed rotations.

[40] For this analysis, we divide the fold-thrust belt of the Bolivian Andes into three regions from hinterland to foreland: the Altiplano, the Eastern Cordillera, and the combined Subandean and Interandean zones. North of the axis of curvature of the Bolivian Orocline (Figure 12a), estimates of crustal shortening within the Subandean and Interandean zones are provided by *Baby et al.* [1997], *Kley et al.* [1999] and *McQuarrie* [2002b]. For a profile centered at 17°S, 66°W, *McQuarrie* [2002b] determined a shortening of 111 km. *Baby et al.* [1997] estimate shortening of 74 km between 15° and 16°S. *Kley et al.* [1999] indicate that shortening was ~20 km across the Subandean and Interandean zones near the Madre de Díos basin at 13°S, 72°W. The resulting Euler rotation is ~6° counterclockwise about an Euler pole located at 12°S, 74°W (Figure 12b). South of the axis of curvature within the Subandean and Interandean zones, crustal shortening estimates are 163 km at 20°S, 63.5°W [*McQuarrie*, 2002b], 125 km at ~21.5°S, 64°W [*Baby et al.*, 1997], and ~30 km at 24°S, 64.5°W [*Kley et al.*, 1999]. The resulting Euler rotation is 18° clockwise about an Euler pole located at 24.5°S, 64°W (Figure 12b).

[41] Within the Eastern Cordillera south of the curvature axis, crustal shortening of 122 km was determined by *McQuarrie* [2002b] at 19.5°S, 66°W. *Baby et al.* [1997] estimate shortening of 86 km at 21.5°S, 66°W. Along a profile centered at 25°S, 65°W, *Kley et al.* [1999] estimated a total of 45–70 km shortening across the combined Santa Barbara System and Eastern Cordillera. These authors estimated 30 km of shortening within the Santa Barbara System with the remaining 15–40 km shortening assigned to the Eastern Cordillera. We use an estimate of 30 km shortening within the Eastern Cordillera along this profile. These shortening estimates indicate a clockwise Euler rotation of 8° about a pole at 27°S, 65°W for the Eastern Cordillera south of the curvature axis (Figure 12c). In the Eastern Cordillera north of the axis, crustal shortening estimates are 142 km at 18°S, 66.5°W [*McQuarrie*, 2002b] and 103 km at ~17°S, 68°W [*Baby et al.*, 1997]. The proximity of these two cross sections do not provide control on the location of the Euler pole location independent of the Euler pole location calculated for the Subandean and Interandean zones. We thus use the latter pole to calculate a counterclockwise Euler rotation of 8° for the Eastern Cordillera north of the axis (Figure 12c).

[42] In the Corque syncline area (18.5°S, 68°W) within the Altiplano north of the curvature axis, *McQuarrie* [2002b] determined a shortening of 47 km during the past 15 m.y. South of the curvature axis at 20°S, 67°W, *McQuarrie* [2002b] determined a post-15 Ma shortening of 41 km. Estimates of shortening within the Altiplano by *Baby et al.* [1997] are much less at 14 km (18°S, 69°W) and 20 km (21.5°S, 67°W). We use an intermediate value between these estimates to arrive at Neogene Euler pole rotations of 2° counterclockwise and clockwise for the Altiplano north and south of the curvature axis, respectively (Figure 12b). The sequence of Euler rotations and a first-order reconstruction of the Bolivian Andes over the past 35 m.y. implied by along-strike variations in crustal shortening are summarized in Figure 12. This reconstruction is

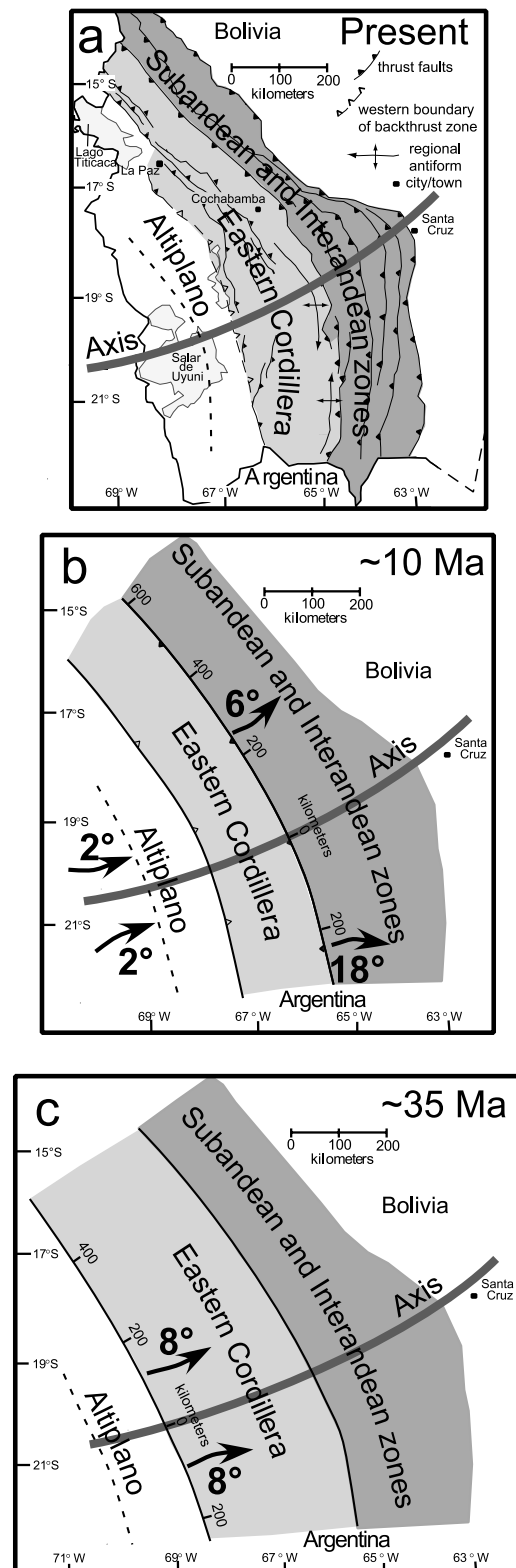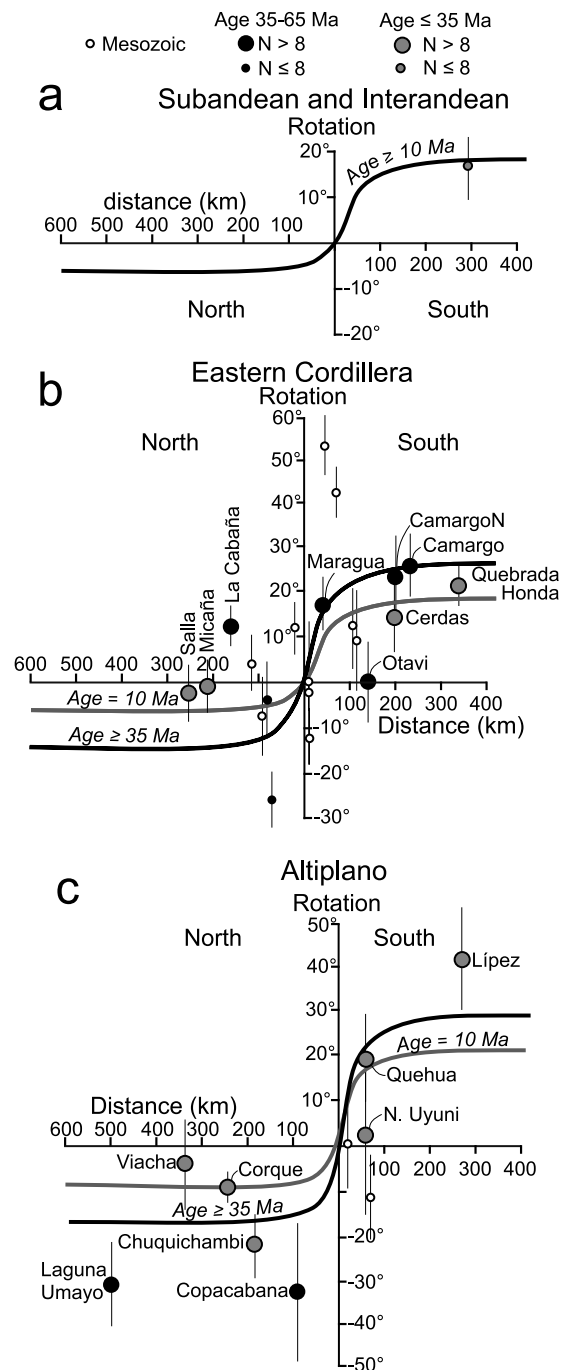

Figure 12. Retrodeformation and vertical-axis rotations within the Bolivia Andes. (a) Present configuration of Bolivian Andes. Axis of Bolivian Orocline is shown by bold gray line. (b) Vertical-axis rotations that occurred after 10 Ma are indicated by arrows with rotation value. (c) Vertical-axis rotations that occurred between ~35 Ma and 10 Ma are indicated by arrows with rotation value.

admittedly crude. In detail, crustal shortening within the Eastern Cordillera overlaps in time with shortening in the Subandean and Interandean zones. Also shortening and rotations vary within these belts such that the amount of rotation experienced by a particular rock unit depends on age of rock and location within each belt. In addition, rotations are surely segmented into smaller crustal domains separated by transfer zones as suggested by *Müller et al.* [2002]. However, given the substantial uncertainties in amounts and timing of crustal shortening, the predictions of vertical-axis rotations from the simple Euler rotation model described here are useful for comparison to paleomagnetic determinations of vertical-axis rotation (Figure 13).

[43] The Euler pole analysis described above was used to predict the vertical-axis rotations for rocks of different ages within the Altiplano, Eastern Cordillera, and combined Subandean and Interandean zones. The width of the transition from clockwise rotations south of the curvature axis to counterclockwise to the northwest was estimated from the distance over which fold axes and faults change strike through the axis of curvature. Vertical-axis rotations determined from paleomagnetism of Mesozoic and Cenozoic rocks of the Bolivian Andes are tabulated in Tables 1 and 2 and are illustrated in Figure 13a for the Subandean and Interandean zones, in Figure 13b for the Eastern Cordillera, and in Figure 13c for the Altiplano.

[44] The major episodes of fold-thrust belt development occurred during the mid-Tertiary and Neogene. To most clearly discern vertical-axis rotations produced by fold-thrust belt development, the best approach is to examine vertical-axis rotations experienced by rocks that immediately predate development of the fold-thrust belt. It is much less effective to test the Euler rotation model using apparent vertical-axis rotations determined from paleomagnetism of Mesozoic units. This is in part because the primary origin of the characteristic magnetization for at least some of the Mesozoic units is questionable (see discussion of regional inclination-only fold test above). In addition, apparent ver-

tical-axis rotations determined from paleomagnetism of Mesozoic units include effects of deformations predating development of the fold-thrust belt that the Euler rotations are intended to model. Observed vertical-axis rotations for Mesozoic units are illustrated in Figures 13b and 13c and it is apparent that rotations from Mesozoic units within the Eastern Cordillera do not fit the model rotations. As noted by *Butler et al.* [1995], the large (43.0° ± 5.8°) clockwise rotation at La Palca (locality 14 of Table 1) is probably due to drag folding along the NE-striking Khenayani-Turuchipa paleostructural corridor (CPKT) [*Sempere et al.*, 1997]. The large clockwise rotation observed for the Aroifilla Formation near Chaunaca is likely due to local noncylindrical folding of uncertain age while tectonic explanations

Figure 13. Models of vertical-axis rotations resulting from along-strike variations in crustal shortening. (a) Rotation predicted by Euler rotations within Subandean and Interandean zones occurred since ∼10 Ma and affected all rocks with ages ≥10 Ma. (b) Rotation curves predicted by Euler rotations within the Eastern Cordillera. Rotation curve predicted for rocks ≤10 Ma is shown by gray line while rotations predicted for rocks ≥35 Ma are shown by black line. (c) Rotation curves predicted by Euler rotations within the Altiplano. Rotation curve predicted for rocks ≤10 Ma is shown by gray line while rotations predicted for rocks ≥35 Ma are shown by black line. Observed rotations determined from paleomagnetic analyses are shown by black circles for rocks with age 35–65 Ma (smaller circles for results based on ≤8 paleomagnetic sites). Rotations determined from paleomagnetic analyses of rocks with age ≤35 Ma are shown by gray circles (smaller circles for results based on ≤8 paleomagnetic sites). Rotations determined from paleomagnetic analyses of Mesozoic rocks are shown by small open circles. Vertical bars through rotation values indicate 95% confidence limits on amount of vertical-axis rotation.

for rotations experienced at other Mesozoic localities are not readily apparent.

[45] Comparing paleomagnetic determinations of vertical-axis rotations from Cenozoic rocks with the model rotations provide the best opportunity to test the Euler rotation model. Cenozoic strata from which N > 8 sites were used to compute the rotation provide the most reliable determinations of vertical-axis rotation and larger symbols are used in Figure 13 to illustrate these rotations. Certainly any model for vertical-axis rotations should at least accurately predict the most reliable observed rotations in the region of the most straightforward geology. As shown in Figure 13a, the single determination of vertical-axis rotation from Neogene rocks of the southern Subandean zone does fit the model prediction of ~18° clockwise rotation. The important result is that a clockwise rotation of almost 20° is predicted for the southern Subandean and Interandean zones by along-strike variation in crustal shortening and the predicted sense and amount of rotation is in fact observed in this region of the Bolivian Andes. Unfortunately there are no reliable paleomagnetic results available for the Subandean and Interandean zones north of the axis of curvature.

[46] There are four paleomagnetic results from Neogene rocks of the Eastern Cordillera that provide tests of the Euler rotation model (Table 2). These observed vertical-axis rotations reasonably fit the rotations predicted to have occurred since 10 Ma (Figure 13b). The paleomagnetic results from Cerdas and Quebrada Honda are consistent with the predicted 18° clockwise rotation produced by along-strike variation in crustal shortening within the inboard Subandean and Interandean zones. Observed rotations at Salla and Micaña in the northern part of the Eastern Cordillera are less than but not significant from the predicted 6° counterclockwise rotation.

[47] There are seven paleomagnetic results from Paleogene rocks of the Eastern Cordillera and five of the observed rotation values are based on N > 8 sites (Table 1). Results from Camargo (localities 19 and 20) and Maragua (locality 12) match the predicted rotations for this belt south of the curvature axis (Figure 13b). The Camargo Syncline is a prominent structure in southern Bolivia and is aligned with the regional strike over a north-south distance >100 km. The predicted clockwise rotation of 26° is matched by the observed rotations of 26.5° ± 7.2° and 24.2° ± 8.9° from Camargo and Camargo North, respectively. The observed clockwise rotation of 17.9° ± 6.0° for the Maragua Syncline agrees with the predicted rotation in this area 50 km south of the axis of curvature of the Bolivian Andes.

[48] Two reliably determined rotations of 35–65 Ma rocks within the Eastern Cordillera do not fit the pattern predicted by the Euler rotation model (Figure 13b). The strike of the Otavi Syncline fold axis is ~30° counterclockwise from the regional trend; compare the orientation of the Otavi and Camargo synclines (localities 17 and 20 in Figure 11). The observed Otavi Syncline rotation (0.2° ± 9.1°) is ~26° counterclockwise from the predicted rotation. We interpret the incongruent orientation of the Otavi Syncline and the mismatch between observed and predicted vertical-axis rotations to be the result of a local counterclockwise rotation that affected an area of 10 to 20 km dimension. Similarly, a local clockwise rotation is required

to explain the mismatch between the observed 12.8° ± 4.5° clockwise rotation and the predicted 15° counterclockwise rotation at La Cabaña (locality 1) near Cochabamba. We agree with *Lamb* [2001a] that the Cochabamba Basin and adjacent areas are probably complicated by local rotations in both clockwise and counterclockwise directions. Apparently, along-strike variations of fold-thrust shortening within the Eastern Cordillera are sufficient to explain vertical-axis rotations of areas with relatively uncomplicated deformation histories but additional local block rotations are required in more complex areas.

[49] Deformations of a wide range of ages have affected the Altiplano and complexities of the deformation history are hidden beneath Neogene deposits. Not surprisingly, the Euler rotation model largely fails to explain the observed vertical-axis rotations within the Altiplano (Table 2). Rotations for the ≤30 Ma units at Quehua, Viacha, and the Corque Syncline are reasonably fit by Euler rotations since 10 Ma (Figure 13c). However, rotations at Lípez, North Uyuni, and Chuquichambi require additional local rotations as interpreted by *Roperch et al.* [2000]. The paleomagnetic determinations of vertical-axis rotations for ~60 Ma rocks at Laguna Umayo and Copacabana (Table 1 and Figure 13c) far exceed those predicted by the Euler rotation model. While the Euler rotation model of along-strike variations in crustal shortening within the Bolivian fold-thrust belt reasonably explains the paleomagnetic determinations of vertical-axis rotation within the Eastern Cordillera and the Subandean and Interandean zones, vertical-axis rotations within the Altiplano are dominated by local rotations of crustal blocks.

References

Baby, P., P. Rochat, G. Mascle, and G. Hérail (1997), Neogene shortening contribution to crustal thickening in the back arc of the Central Andes, *Geology*, 25, 883–886.

Beck, M. E. (1980), Paleomagnetic record of plate-margin tectonics processes along the western edge of North America, *J. Geophys. Res.*, 85, 7115–7131.

Beck, M. E., Jr. (1987), Tectonic rotations on the leading edge of South America: The Bolivian orocline revisited, *Geology*, 15, 806–808.

Beck, M. E., Jr. (1988), Analysis of Late Jurassic-Recent paleomagnetic data from active plate margins of South America, *J. S. Am. Earth Sci.*, 1, 39–52.

Beck, M. E., Jr. (1998), On the mechanism of crustal block rotations in the central Andes, *Tectonophysics*, 299, 75–92.

Beck, M. E., Jr. (1999), Jurassic and Cretaceous apparent polar wander relative to South America: Some tectonic implications, *J. Geophys. Res.*, 104, 5063–5067.

Beck, M. E., Jr., R. F. Burmester, R. E. Drake, and P. D. Riley (1994), A tale of two continents: Some tectonic contrasts between the central Andes and the North American Cordillera, as illustrated by their paleomagnetic signatures, *Tectonics*, 13, 215–224.

Beck, S., G. Zandt, S. C. Myers, T. C. Wallace, P. G. Silver, and L. Drake (1996), Crustal-thickness variations in the central Andes, *Geology*, 24, 407–410.

Besse, J., and V. Courtillot (2002), Apparent and true polar wander and the geometry of the geomagnetic field over the past 200 Myr, *J. Geophys. Res.*, *107*(B11), 2300, doi:10.1029/2000JB000050.

Bevis, S., E. Kendrick, R. Smalley Jr., B. Brooks, R. Allmendinger, and B. Isacks (2001), On the strength of interplate coupling and the rate of back arc convergence in the central Andes: An analysis of the interseismic velocity field, *Geochem. Geophys. Geosyst.*, *2*, paper number 2001GC000198.

Butler, R. F. (1992), *Paleomagnetism: Magnetic Domains to Geologic Terranes*, 319 pp., Blackwell Sci., Malden, Mass.

Butler, R. F., D. R. Richards, T. Sempere, and L. G. Marshall (1995), Paleomagnetic determinations of vertical-axis tectonic rotations from Late Cretaceous and Paleocene strata of Bolivia, *Geology*, *23*, 799–802.

Cande, S. C., and D. V. Kent (1992), A new geomagnetic polarity time scale for the Late Cretaceous and Cenozoic, *J. Geophys. Res.*, *97*, 13,917–13,951.

Cande, S. C., and D. V. Kent (1995), Revised calibration of the geomagnetic polarity timescale for the Late Cretaceous and Cenozoic, *J. Geophys. Res*, *100*, 6093–6095.

Carey, S. W. (1955), The orocline concept in geotectonics, *Proc. R. Soc. Tasmania*, *89*, 255–288.

DeCelles, P. G., and B. K. Horton (2003), Early to middle Tertiary foreland basin development and the history of Andean crustal shortening in Bolivia, *Geol. Soc. Am. Bull.*, *115*, 58–77.

Demarest, H. H. (1983), Error analysis of the determination of tectonic rotation from paleomagnetic data, *J. Geophys. Res.*, *88*, 4321–4328.

Enkin, R. J., and G. S. Watson (1996), Statistical analysis of palaeomagnetic inclination data, *Geophys. J. Int.*, *126*, 495–504.

Fisher, R. A. (1953), Dispersion on a sphere, *Proc. R. Soc. London, Ser. A*, *217*, 295–305.

Gephart, J. (1994), Topography and subduction geometry in the central Andes: Clues to the mechanics of a noncollisional orogen, *J. Geophys. Res.*, *99*, 12,279–12,288.

Gilder, S., S. Rousse, D. Farber, B. McNulty, T. Sempere, V. Torres, and O. Palacios (2003), Post-Middle Oligocene origin of paleomagnetic rotations in Upper Permian to Lower Jurassic rocks from northern and southern Peru, *Earth Planet. Sci. Lett.*, *210*, 233–248.

Husson, L., and T. Sempere (2003), Thickening the Altiplano crust by gravity-driven crustal channel flow, *Geophys. Res. Lett.*, *30*(5), 1243, doi:10.1029/2002GL016877.

Isacks, B. L. (1988), Uplift of the central Andean plateau and bending of the Bolivian orocline, *J. Geophys. Res.*, *93*, 3211–3231.

Kirschvink, J. L. (1980), The least-squares line and plane and the analysis of paleomagnetic data, *Geophys. J. R. Astron. Soc.*, *62*, 699–718.

Kley, J. (1999), Geologic and geometric constraints on a kinematic model of the Bolivian orocline, *J. South Am. Earth Sci.*, *12*, 221–235.

Kley, J., and C. R. Monaldi (1998), Tectonic shortening and crustal thickening in the Central Andes: How good is the correlation?, *Geology*, *26*, 723–726.

Kley, J., C. R. Monaldi, and J. A. Salfity (1999b), Along-strike segmentation of the Andean foreland: Causes and consequences, *Tectonophysics*, *301*, 75–94.

Lamb, S. (2001a), Vertical axis rotation in the Bolivian orocline, South America. 1. Paleomagnetic analysis of Cretaceous and Cenozoic rocks, *J. Geophys. Res.*, *106*, 26,605–26,632.

Lamb, S. (2001b), Vertical axis rotation in the Bolivian orocline, South America. 2. Kinematic and dynamical implications, *J. Geophys. Res.*, *106*, 26,633–26,653.

Libarkin, J. C., R. F. Butler, D. R. Richards, and T. Sempere (1998), Tertiary remagnetization of Paleozoic rocks from the Eastern Cordillera and Sub-Andean Belt of Bolivia, *J. Geophys. Res.*, *103*, 30,417–30,429.

MacFadden, B. J., F. Anaya, H. Perez, C. W. Naeser, P. K. Zeitler, and K. E. Campbell (1990), Late Cenozoic paleomagnetism and chronology of Andean basins of Bolivia: Evidence for possible oroclinal bending, *J. Geol.*, *94*, 541–555.

MacFadden, B. J., F. Anaya, and C. C. Swisher III (1995), Neogene paleomagnetism and oroclinal bending of the central Andes of Bolivia, *J. Geophys. Res.*, *100*, 8153–8167.

Marshak, S. (1988), Kinematics of orocline and arc formation in thin-skinned orogens, *Tectonics*, *7*, 73–86.

May, S. R., and R. F. Butler (1985), Paleomagnetism of the Puente Piedra Formation, central Peru, *Earth Planet. Sci. Lett.*, *72*, 205–218.

McFadden, P. L. (1990), A new fold test for palaeomagnetic studies, *Geophys. J. Int.*, *103*, 163–169.

McFadden, P. L., and M. W. McElhinny (1990), Classification of the reversal test in palaeomagnetism, *Geophys. J. Int.*, *103*, 725–729.

McQuarrie, N. (2002a), Initial plate geometry, shortening variations, and evolution of the Bolivian orocline, *Geology*, *30*, 867–870.

McQuarrie, N. (2002b), The kinematic history of the central Andean fold-thrust belt, Bolivia: Implications for building a high plateau, *Geol. Soc. Am. Bull.*, *114*, 950–963.

Müller, J. P., J. Kley, and V. Jacobshagen (2002), Structure and Cenozoic kinematics of the Eastern Cordillera, southern Bolivia (21°S), *Tectonics*, *21*(5), 1037, doi:10.1029/2001TC001340.

Randall, D. E. (1998), A new Jurassic-Recent apparent polar wander path for South America and a review of central Andean tectonic models, *Tectonophysics*, *299*, 49–74.

Randall, D. E., A. J. Tomlinson, and G. K. Taylor (2001), Paleomagnetically defined rotations from the Precordillera of northern Chile: Evidence of localized in situ fault-controlled rotations, *Tectonics*, *20*, 235–254.

Roperch, P., and G. Carlier (1992), Paleomagnetism of Mesozoic rocks from the central Andes of southern Peru: Importance of rotations in the development of the Bolivian Orocline, *J. Geophys. Res.*, *97*, 17,233–17,249.

Roperch, P., G. Hérail, and M. Fornari (1999), Magnetostratigraphy of the Miocene Corque basin, Bolivia: Implications for the geodynamic evolution of the Altiplano during the late Tertiary, *J. Geophys. Res.*, *104*, 20,415–20,429.

Roperch, P., M. Fornari, G. Hérail, and G. V. Parraguez (2000), Tectonic rotations within the Bolivian Altiplano: Implications for the geodynamic evolution of the central Andes during the late Tertiary, *J. Geophys. Res.*, *105*, 795–820.

Rousse, S., S. Gilder, D. Farber, B. McNulty, and V. R. Torres (2002), Paleomagnetic evidence for rapid vertical-axis rotation in the Peruvian Cordillera ca. 8 Ma, *Geology*, *30*, 75–78.

Sempere, T., R. F. Butler, D. R. Richards, L. G. Marshall, W. Sharp, and C. C. Swisher III (1997), Stratigraphy and chronology of Upper Cretaceous-lower Paleogene strata in Bolivia and northwest Argentina, *Geol. Soc. Am. Bull.*, *109*, 709–727.

Sempere, T., et al. (2002), Late Permian-Middle Jurassic lithospheric thinning in Peru and Bolivia, and its bearing on Andean-age tectonics, *Tectonophysics*, *345*, 153–181.

Sigé, B., T. Sempere, R. F. Butler, L. G. Marshall, and J.-Y. Crochet (2004), Age and stratigraphic reassessment of the fossil-bearing Laguna Umayo red mudstone unit, SE Peru, from regional stratigraphy, fossil record, and paleomagnetism, *Geobios*, in press.

Somoza, R. (1998), Updated Nazca (Farallon)-South America relative motions during the last 40 My; implications for mountain building in the Central Andean region, *J. S. Am. Earth Sci.*, *11*, 211–215.

Somoza, R., and A. J. Tomlinson (2002), Paleomagnetism in the Precordillera of northern Chile (22°30′S); implications for the history of tectonic rotations in the Central Andes, *Earth Planet. Sci. Lett.*, *194*, 369–381.

Somoza, R., S. Singer, and B. Coira (1996), Paleomagnetism of upper Miocene ignimbrites at the Puna: An analysis of vertical-axis rotations in the Central Andes, *J. Geophys. Res.*, *101*, 11,387–11,400.

Somoza, R., S. Singer, and A. J. Tomlinson (1999), Paleomagnetic study of upper Miocene rocks from northern Chile: Implications for the origin of late Miocene-Recent tectonic rotations in the southern Central Andes, *J. Geophys. Res.*, *104*, 22,923–22,936.

Watson, G. S., and R. J. Enkin (1993), The fold test in paleomagnetism as a parameter estimation problem, *Geophys. Res. Lett.*, *20*, 2135–2137.

Yuan, X., S. V. Sobolev, and R. Kind (2002), Moho topography in the central Andes and its geodynamic implications, *Earth Planet. Sci. Lett.*, *199*, 389–402.

R. F. Butler, Department of Chemistry and Physics, University of Portland, Portland, OR 97203, USA. (butler@up.edu)

D. R. Richards, Midland Valley Inc., 1767A Denver West Blvd, #39, Golden, CO 80401, USA.

T. Sempere, Laboratoire des Mécanismes et Transferts en Géologie, Université Paul Sabatier, Toulouse III, 118, Route de Narbonne, F-31062 Toulouse cedex 4, France. (Thierry.sempere@lmtg.obs-mip.fr)